

Effect of correlations on the thermal equilibrium and normal modes of a non-neutral plasma

Daniel H. E. Dubin

Department of Physics, University of California at San Diego, La Jolla, California 92093-0319

(Received 2 June 1995)

Recent experiments have trapped small spheroidal clouds of like charges, and have cooled them to cryogenic temperatures where strong correlation effects, such as transitions to crystalline states, have been observed. The experiments have also excited normal modes of oscillation in the charge clouds. The normal modes have previously been considered theoretically using a cold-fluid model that neglects correlations. This paper examines the effect of strong correlation on the equilibrium and on the modes. Two correlation effects are predicted to cause frequency shifts in the modes: correlation pressure changes the shape and density of the equilibrium, and bulk and shear moduli introduce restoring forces neglected in the fluid theory. A viscoelastic model of the plasma incorporating these effects is solved perturbatively to obtain formulas for the frequency shifts. [S1063-651X(96)03905-0]

PACS number(s): 52.25.Wz, 32.80.Pj, 52.35.Fp, 62.20.Dc

I. INTRODUCTION

Non-neutral plasmas, which are composed only of charges of like sign, possess two intriguing properties: they can be confined using electromagnetic fields for long periods of time (i.e., hours or even days); and they can be cooled without recombination to ultralow temperatures (on the order of mK or less), where states of condensed matter such as non-neutral liquids and crystals are observed. In these strongly correlated non-neutral plasmas the interparticle spacings are typically microns or larger, so that densities are over ten orders of magnitude less than conventional condensed matter.

The collective electrostatic modes of oscillation of non-neutral plasmas have recently received considerable attention for a number of reasons. Excitation and measurement of the collective modes can provide a useful nondestructive diagnostic of such plasma properties as density and temperature, as well as the shape and overall size of the plasma [1–4]. Modes have also been implicated in transport processes leading to loss of the plasma and limits on the density [1,5]. Furthermore, when the plasma is small compared to the size of the trapping electrodes, an analytic theory exists that provides a complete solution for all of the modes [6].

However, this analytic theory neglects the effect of correlations and treats the plasma as a cold fluid. In this paper we consider how interparticle correlations can affect the normal modes in a strongly correlated trapped plasma. Here we will consider a theoretical model that describes correlation effects on the modes; in another paper [7], we will test the theory by comparing its predictions for the mode frequencies to the results of molecular-dynamics (MD) simulations. We have two related reasons for pursuing this analysis: we wish to understand to what extent the crystallization of the trapped plasma affects the normal modes, and, given that there are measurable effects, we will consider what information a measurement of the modes can provide concerning correlation properties of the plasma.

The theory developed in this paper consists of a perturbative solution of a viscoelastic model for the correlated plasma. In addition to the usual electromagnetic forces acting

on the non-neutral plasma, a pressure tensor is introduced to the equations of motion in order to account for the effect of thermal pressure on the equilibrium and dynamics. The theory differs from previous studies of correlation effects on plasma waves in that the finite size of the trapped plasma is explicitly taken into account. This is an important aspect for comparisons to actual experiments and simulations of low-order modes in small trapped plasmas, for which the mode wavelength is of order the size of the plasma.

Mode frequencies are found to shift compared to the cold-fluid theory of Ref. [6] (where pressure is neglected). The shift can be traced to two effects of approximately equal magnitude: (i) the equilibrium shape and density of the trapped plasma are changed by thermal pressure, causing a shift in the mode frequencies; and (ii) extra restoring forces due to bulk and shear moduli of the strongly correlated plasma also lead to frequency shifts. For several of the modes explicit formulas are derived for the frequency shifts.

The paper is structured in the following manner. In Sec. II, after a brief review of the thermal equilibrium properties of trapped non-neutral plasmas, an analytic theory is developed in order to predict the effect of thermal and correlation pressure on the plasma equilibrium. Correlations are found to affect polynomial moments of the equilibrium plasma density. The analytic predictions for these moments are compared to computer simulations of equilibrium plasmas, and good agreement is found.

In Sec. III we briefly review the theory for the normal modes of a cold-fluid plasma, and then we go on to introduce and solve our viscoelastic model of the correlated plasma modes. It turns out that the perturbative solution of this model requires the polynomial moments of the equilibrium density which were derived in Sec. II. Thus, analytic forms for the correlation frequency shifts of the modes can be derived. Section IV is devoted to a summary and discussion of the results. In Appendix A we derive an intermediate result required for the theory of pressure effects on the plasma equilibrium. In Appendix B we perform several tests of the perturbation theory developed to solve the viscoelastic model. We first consider the perturbed potential eigenfunction in order to test the convergence of the theory. We then

compare the perturbation solution to an exact solution of the viscoelastic model for a special case.

II. EQUILIBRIUM PROPERTIES

In this section we review the static thermal equilibrium properties of a single species plasma confined in a Penning or Paul trap. We then go on to derive some results for density moments of a thermal equilibrium plasma. We will need these results for our treatment of normal modes of the trapped plasma.

A. Gibb's distribution in a harmonic trap

It is possible to trap a collection of charges of like sign for long periods of time, so that the collection approaches a state of confined thermal equilibrium. The thermal equilibrium state is determined by the constants of the motion. In a Penning trap [8] the uniform confining magnetic field and the applied electric field are nominally static and cylindrically symmetric so the energy H and the component of angular momentum along the trap axis P_z are conserved quantities. The angular momentum has both kinetic and magnetic components

$$P_z = M \sum_{i=1}^N (v_{\theta i} \rho_i + \Omega_c \rho_i^2 / 2),$$

where $\Omega_c = qB/Mc$ is the cyclotron frequency, q is the charge, M the mass, B the magnetic field strength, and c is the speed of light. Cylindrical coordinates $\mathbf{x} = (\rho, \theta, z)$ are employed, measured with respect to the center of the trap, with z oriented along the axis of symmetry. The energy H is

$$H = \sum_{i=1}^N \left\{ \frac{1}{2} M v_i^2 + q \phi_T(\mathbf{x}_i) + \sum_{j>i} \phi_{ij} \right\},$$

where ϕ_{ij} is the interaction potential energy between particles i and j , and $\phi_T(\mathbf{x})$ is the external trap potential due to the voltages imposed on the electrodes. For plasmas which are small compared to the trap electrodes, image charges can be neglected, $\phi_{ij} = q^2/|\mathbf{x}_i - \mathbf{x}_j|$, and ϕ_T is well approximated by its Taylor expansion over the small central region where the plasma is trapped:

$$\phi_T(\mathbf{x}) = \frac{M \omega_z^2}{2q} (z^2 - \rho^2/2),$$

where ω_z is the frequency of axial oscillatory motion when a single charge is confined. Traps with such an external trap potential are referred to as "harmonic." In order to avoid unessential mathematical complications, this paper focuses on plasmas in harmonic traps.

In a Paul trap [9] there is no magnetic field, and confinement is provided by a combination of electrostatic potentials and electric fields varying at radio frequencies. The latter fields induce a fast rf jitter motion of the ions which, when averaged, leads to a ponderomotive confining potential. If the small amplitude fast jitter motion is neglected and only the ponderomotive potential $\phi_{PD}(\mathbf{x})$ is kept, the resulting dynamics is conservative, with energy

$$H = \sum_{i=1}^N \left\{ \frac{1}{2} M v_i^2 + q \phi_{PD}(\mathbf{x}_i) + \sum_{j>i} \phi_{ij} \right\}.$$

Here again when the plasma is small compared to the distance to the electrodes, ϕ_{PD} is harmonic:

$$\phi_{PD}(\mathbf{x}) = \frac{M}{2q} (\omega_z^2 z^2 + \omega_{\perp}^2 \rho^2),$$

where ω_{\perp} is the frequency of radial oscillations of a single particle in the trap. Note that both ω_z and ω_{\perp} must be small compared to the rf drive frequency in order to use the ponderomotive potential approximation. The angular momentum is also conserved in cylindrically symmetric Paul traps:

$$P_z = \sum_{i=1}^N M v_{\theta i} \rho_i.$$

For both the Penning and Paul traps the thermal equilibrium can then be described in a unified manner. The conserved energy H and angular momentum P_z imply the existence of a confined thermal equilibrium state, described by the Gibb's distribution

$$f(\mathbf{x}_1 \dots \mathbf{x}_N, \mathbf{v}_1 \dots \mathbf{v}_N) = Z^{-1} \exp[-(H - \omega_r P_z)/kT],$$

where ω_r is the rotation frequency of the plasma, Z^{-1} is a constant that normalizes the phase-space integral of f to unity, and T is the temperature. In a Paul trap the rotation frequency ω_r is usually taken to be zero, but in a Penning trap plasma rotation is essential for confinement.

For both types of trap the Gibb's distribution can be rewritten as a product of a Maxwellian velocity distribution, shifted by the rotation frequency ω_r , and a configurational distribution:

$$f = Z^{-1} \exp \left[-M \sum_i (\mathbf{v}_i - \omega_r \rho_i \hat{\theta}_i)^2 / 2kT \right] \times \exp \left[- \sum_i \left\{ \sum_{j<i} \phi_{ij} + q \phi_e(\mathbf{x}_i) \right\} / kT \right], \quad (2.1a)$$

where, for a harmonic trap,

$$\phi_e(\mathbf{x}) = \frac{M \omega_z^2}{2q} (z^2 + \beta \rho^2) \quad (2.1b)$$

is the effective confinement potential that traps the plasma. The parameter β , referred to as the trap parameter, must be greater than zero in order for the plasma to be confined. In a Penning trap β is

$$\beta = - \frac{\omega_r (\Omega_c + \omega_r)}{\omega_z^2} - \frac{1}{2}. \quad (2.2a)$$

This shows that in a Penning trap rotation through the magnetic field ($\omega_r \Omega_c < 0$) is required for particle confinement, but in a Paul trap rotation is not required. In the Paul trap

$$\beta = \frac{\omega_{\perp}^2 - \omega_r^2}{\omega_z^2}, \quad (2.2b)$$

but rotation is generally a negligible effect in Paul traps so one often takes $\beta = \omega_{\perp}^2 / \omega_z^2$.

B. Cold-fluid equilibrium

The thermal equilibrium properties of either harmonic Penning or Paul trap plasmas are described by the same Gibb's distribution function, Eq. (2.1a), with the same effective confinement potential ϕ_e , Eq. (2.1b). This potential, along with the total particle number N and temperature T , uniquely determines the equilibrium density. For example, the Laplacian of $\phi_e(\mathbf{x})$ is constant, and can be related to a constant density n_0 through Poisson's equation

$$n_0 = \frac{1}{4\pi q} \nabla^2 \phi_e = \frac{M \omega_z^2}{4\pi q^2} (2\beta + 1). \quad (2.3)$$

One can think of ϕ_e as being produced by a uniform neutralizing background charge of density n_0 . At low temperatures the plasma minimizes its energy by matching its density to n_0 . Thus, if one neglects density variations on the scale of an interparticle spacing (i.e., if one neglects correlations), the low temperature plasma has uniform density n_0 , out to a surface of revolution where the supply of charge is exhausted. This approximation is referred to as the cold-fluid equilibrium.

Furthermore, Eq. (2.1b) implies that the shape of this surface of revolution is determined solely by the trap parameter β . For example, when $\beta = 1$ the plasma is a sphere, whereas for small β the fluid plasma flattens into a disc and for large β the plasma approaches a line. In fact, it has been shown that, for low temperatures $T \rightarrow 0$, the fluid plasma in a harmonic trap is a spheroid (ellipsoid of revolution). This follows because the electrostatic plasma potential within a uniform spheroid is related to its shape and density by [10]

$$\phi_p = -\frac{1}{4} \frac{M \omega_p^2}{q} [A_1(\alpha) \rho^2 + A_3(\alpha) z^2 - 2A_1(\alpha) R^2 - A_3(\alpha) L^2], \quad (2.4)$$

where $\omega_p^2 = 4\pi q^2 n_0 / M$ is the plasma frequency. Here we introduce the aspect ratio α of the spheroid, which equals the length $2L$ of the spheroid divided by the diameter $2R$. The functions of the aspect ratio $A_1(\alpha)$ and $A_3(\alpha)$ are

$$A_1(\alpha) = \frac{1 - e^2}{e^2} \left[\frac{1}{1 - e^2} - \frac{1}{2e} \ln \left(\frac{1 + e}{1 - e} \right) \right], \quad (2.5a)$$

$$A_3(\alpha) = 2 - 2A_1(\alpha), \quad (2.5b)$$

where $e^2 = 1 - 1/\alpha^2$. In equilibrium at zero temperature the plasma potential ϕ_p must match the effective confining potential $\phi_p + \phi_e = \text{const}$ within the plasma. This equation, together with Eqs. (2.1b) and (2.4), leads to the following relation between the trap parameter and the plasma aspect ratio:

$$\beta = A_1(\alpha) / A_3(\alpha). \quad (2.6)$$

The size of a plasma of given aspect ratio is determined by the total particle number N , and the density n_0 . This follows

from the relation between the spheroid volume and N : $\frac{4}{3} \pi L R^2 n_0 = N$, which can be rewritten in terms of the Wigner-Seitz radius a_{WS} and the aspect ratio α :

$$\left(\frac{L}{a_{\text{WS}}} \right)^3 = N \alpha^2, \quad \left(\frac{R}{a_{\text{WS}}} \right)^3 = \frac{N}{\alpha}. \quad (2.7)$$

(The Wigner-Seitz radius is the average interparticle spacing, defined in terms of n_0 by $4\pi a_{\text{WS}}^3 n_0 / 3 = 1$.) Equations (2.6) and (2.7) have been verified experimentally in low temperature Penning trap experiments [11].

C. Cold-fluid moments

In Sec. III we will require moments of the cold-fluid plasma density when we consider the normal modes. We will need moments of the form

$$\langle z^{2l} \rho^{2m} \rangle_f \equiv \frac{1}{N} \int d^3x n_f(\mathbf{x}) z^{2l} \rho^{2m}$$

for integers l and m , where the subscript f on the average indicates a moment taken with respect to the cold-fluid plasma, and $n_f(\mathbf{x})$ is the cold-fluid plasma density, equal to n_0 within the plasma and zero outside of the plasma. The integrals over $n_f(\mathbf{x})$ could in principle be determined numerically for a plasma of any shape, but for a spheroidal plasma the moments can be determined analytically. The required integrals are over the interior of a spheroid whose surface is defined by $z^2/L^2 + \rho^2/R^2 = 1$, and the result is

$$\langle z^{2l} \rho^{2m} \rangle_f = \frac{3}{4} \frac{\Gamma(m+1) \Gamma(l+1/2)}{\Gamma(l+m+5/2)} L^{2l} R^{2m}, \quad (2.8)$$

where $\Gamma(x)$ is a gamma function.

D. Thermal equilibrium correlations

We now turn to the effects of finite temperature and correlations on the equilibrium. Equation (2.3) implies that the effective confinement potential can be thought of as being produced by a uniform background density n_0 . A system of charges confined in such a static background is termed a one-component plasma (OCP). Thus the Gibb's distribution f of a trapped non-neutral plasma is identical to that of a OCP, except for the shift in velocities due to rotation. The OCP is a paradigm of condensed matter with a long history [12]. The correlation properties of a classical infinite homogeneous OCP are entirely determined by the correlation parameter $\Gamma = q^2 / a_{\text{WS}} kT$. At $\Gamma \cong 2$ the OCP begins to exhibit short-range order characteristic of a liquid [13], and at $\Gamma = 172$ a first-order transition to a bcc lattice is predicted [13,14].

However, in present experiments the trapped plasma typically consists of less than 100 000 charges, so it is neither infinite nor homogeneous, and this affects the correlation properties [15]. In Fig. 1 we plot the density $n(r; \Gamma)$ in a spherical plasma as a function of spherical radius r , for various values of Γ . This density is determined from Metropolis-Rosenbluth Monte Carlo (MC) averages over the Gibb's distribution,

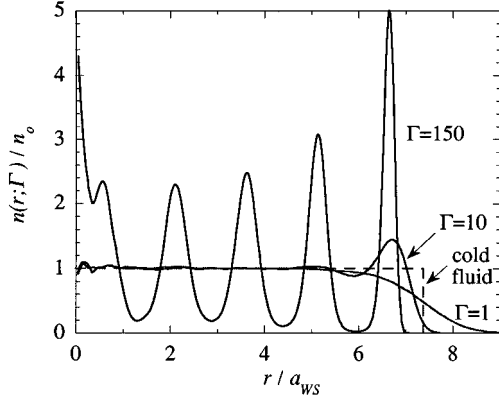


FIG. 1. Equilibrium density $n(r;\Gamma)$ as a function of spherical radius r in a spherically symmetric ($\alpha=\beta=1$) non-neutral plasma of $N=400$ charges trapped in the effective potential of Eq. (2.1b), for various values of the correlation parameter Γ (generated using a Monte Carlo simulation). The density is normalized to the cold-fluid value n_0 . Lengths are measured in units of the Wigner-Seitz radius a_{ws} . The dotted line is the cold-fluid theory, with a sharp edge at $r/a_{ws}=N^{1/3}$ [see Eq. (2.7)]. $\Gamma=1, 10$, and 150 from smoothest to most oscillatory profile.

$n(\mathbf{x}_1;\Gamma)$

$$= N \int d^3x_2 \dots d^3x_N d^3v_1 \dots d^3v_N f(\mathbf{x}_1 \dots \mathbf{x}_N, \mathbf{v}_1 \dots \mathbf{v}_N). \quad (2.9)$$

For relatively small values of the correlation parameter Γ the density is approximately uniform within the plasma, falling to zero at the plasma edge over a distance on the order of the Debye length [16]. As the temperature decreases, the Debye length decreases and the plasma edge steepens, approaching the Heaviside step function density $n_f(\mathbf{x})$ of cold-fluid theory. However, as Γ increases the density also begins to exhibit spatially decaying oscillations (see Fig. 1). As Γ increases beyond about $\Gamma \sim 10^2$ the oscillations increase in magnitude until the density approaches zero between the peaks, and the system forms concentric shells. This concentric shell structure has been observed in experiments [17]. At large Γ values ($\Gamma \gtrsim 300-1000$) the charges in a given shell generally crystallize into a distorted two-dimensional (2D) hexagonal structure, although for extremely oblate or prolate clouds other crystal structures are predicted to occur [18].

These qualitative correlation effects have been discussed in several previous articles. However, in this paper we will be concerned with the effect of correlations on the low-order modes of the plasma. Since these modes have relatively long wavelengths compared to an interparticle spacing, we will find that only average correlation properties are important, in which case some quantitative results can be obtained.

E. Density moments

Moments of the equilibrium density are affected by the correlations. In Fig. 2 we plot the mean-square length $\langle z^2 \rangle = (1/N) \sum_i z_i^2$ for a crystallized plasma of 1000 particles [determined via molecular-dynamics (MD) simulation], as a function of the trap parameter β . On this plot is also shown

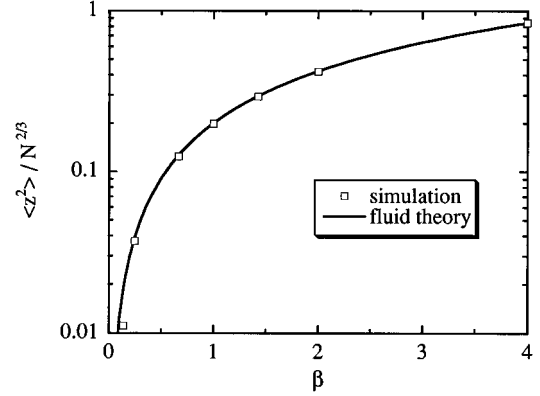


FIG. 2. Mean-square length $\langle z^2 \rangle$ as a function of trap parameter β for $N=1000$ charges. Dots: molecular dynamics simulations of crystallized ($\Gamma \rightarrow \infty$) plasmas. Line: cold-fluid theory [Eqs. (2.6)–(2.8)]. Lengths are measured in units of the Wigner-Seitz radius a_{ws} .

the cold-fluid theory result of Eq. (2.8), $\langle z^2 \rangle_f = L^2/5$. Here L is a function of β and N through Eqs. (2.7) and (2.8). There is a slight difference between the simulation results and the cold-fluid prediction, visible at small β , which can be traced to an effect of correlations. The cold-fluid theory of Eqs. (2.3)–(2.8) neglects the effect of pressure on the density distribution. Here we are referring to the bulk thermal pressure of the infinite homogeneous OCP,

$$p = n_0 k T \left(1 + \frac{1}{3} \frac{U}{NkT} \right), \quad (2.10)$$

where U is the correlation contribution to the internal energy [13]. In the strong correlation regime this pressure is negative because U/NkT is negative. This negative pressure leads to a reduction in the size of the plasma.

Negative pressure, or a net attractive force, may seem counterintuitive in a system of charges interacting via the repulsive Coulomb potential. However, it must be remembered that this negative pressure is an effect *in addition* to the long-range repulsion kept in the mean-field potential ϕ_p of Eq. (2.4); the plasma charges still repel one another, but the repulsion is less than in the fluid limit and so $\langle z^2 \rangle$ is less than the cold-fluid prediction. This correlation effect can also be observed in Fig. 1, where for large Γ the edge of the plasma has shrunk inside the edge predicted by the cold-fluid theory, shown by the dotted line.

Quantitative predictions for the effect of pressure on the density moments can be obtained provided that we make several approximations. We assume that the density is uniform except near the plasma edge, which is assumed to be relatively narrow compared to the plasma dimensions. This is a good approximation for the low Γ profiles pictured in Fig. 1, but for large Γ it is difficult to justify, since shells form throughout the plasma. Nevertheless we will observe that our results for the density moments are in good agreement with computer simulations even for large Γ .

For any function of position $F(\mathbf{x})$ we define a moment $\langle F \rangle$ as an average over the single-particle equilibrium density $n(\mathbf{x};\Gamma)$:

$$\langle F \rangle = \frac{1}{N} \sum_{i=1}^N \langle F(\mathbf{x}_i) \rangle = \frac{1}{N} \int d^3x F(\mathbf{x}) n(\mathbf{x}; \Gamma). \quad (2.11)$$

We then break the moment into two parts:

$$\langle F \rangle = \frac{1}{N} \int d^3x F(\mathbf{x}) n_f(\mathbf{x}) + \frac{1}{N} \int d^3x F(\mathbf{x}) \Delta n(\mathbf{x}),$$

where $\Delta n = n(\mathbf{x}; \Gamma) - n_f(\mathbf{x})$. The first term is the cold-fluid moment $\langle F \rangle_f$ discussed in Sec. II C, and the second term is the correction which we call $\Delta \langle F \rangle$.

Now, by assumption, $n(\mathbf{x}; \Gamma)$ is equal to $n_f(\mathbf{x})$ except near the edge of the plasma, so $\Delta n(\mathbf{x})$ is a highly peaked function of distance from the edge. We therefore Taylor expand $F(\mathbf{x})$ in powers of the distance u from the edge of the cold-fluid plasma. Defining $\mathbf{x} = \mathbf{x}_0$ at the fluid surface,

$$\begin{aligned} \Delta \langle F \rangle &\equiv \langle F \rangle - \langle F \rangle_f = \frac{1}{N} \int d^2x_0 F(\mathbf{x}_0) \int_{-\infty}^{\infty} du \Delta n(u; \Gamma) \\ &+ \frac{1}{N} \int d^2x_0 \hat{\mathbf{u}} \cdot \nabla F(\mathbf{x}_0) \int_{-\infty}^{\infty} duu \Delta n(u; \Gamma), \end{aligned} \quad (2.12)$$

where $\hat{\mathbf{u}}$ is a unit vector normal to the fluid surface, and where we have assumed that $\Delta n(\mathbf{x}; \Gamma)$ is homogeneous along the surface so that it is a function only of u rather than \mathbf{x} (that is, curvature variations in the surface are neglected, which is equivalent to neglecting surface tension effects). The integral $\int_{-\infty}^{\infty} du \Delta n(u; \Gamma)$ vanishes by conservation of total particle number. The second integral over u is evaluated in Appendix A using the equilibrium Bogoliubov-Born-Green-Kirkwood-Yvon (BBGKY) hierarchy, again neglecting surface curvature variations. The result from Eq. (A5) is

$$\int_{-\infty}^{\infty} duu \Delta n(u; \Gamma) = \frac{p}{M \omega_p^2}, \quad (2.13)$$

where p is the bulk pressure of the one-component plasma, given in terms of the correlation contribution to the internal energy by Eq. (2.10).

Using Eq. (2.13) in Eq. (2.12), and using Gauss's theorem for the surface integral, we obtain

$$\Delta \langle F \rangle = \frac{p}{M \omega_p^2 n_0} \langle \nabla^2 F \rangle_f. \quad (2.14)$$

Thus the correction to any density moment due to correlations or thermal effects is proportional to the plasma pressure p . Equation (2.14) applies to a plasma in any trap geometry, not just a harmonic trap. For example, for plasma in any confinement geometry Eq. (2.14) predicts the following correlation changes in the mean-square length and radius:

$$\Delta \langle z^2 \rangle = \frac{2p}{M \omega_p^2 n_0}, \quad \Delta \langle \rho^2 \rangle = \frac{4p}{M \omega_p^2 n_0}.$$

For plasmas in a harmonic trap and for moments of the form $\langle z^{2l} \rho^{2m} \rangle$ the required integral over the fluid spheroid in Eq. (2.14) can be performed analytically, and the result is

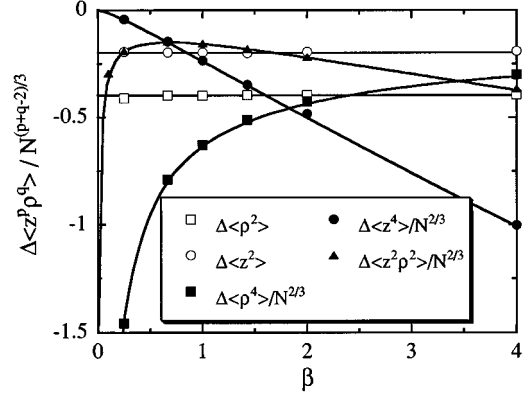


FIG. 3. Difference $\Delta \langle z^{2l} \rho^{2m} \rangle$ between density moments as seen in simulations and fluid theory predictions as a function of trap parameter β , for crystallized plasmas and for various values of l and m . Dots: simulation results. Lines: predictions of Eq. (2.15). Lengths are measured in units of a_{WS} .

$$\Delta \langle z^{2l} \rho^{2m} \rangle = 2 \langle z^{2l} \rho^{2m} \rangle_f (2l + 2m + 3) \left(\frac{l}{L^2} + \frac{m}{R^2} \right) \frac{p}{M \omega_p^2 n_0}, \quad (2.15)$$

where the fluid moment $\langle z^{2l} \rho^{2m} \rangle_f$ is given by Eq. (2.8). Equation (2.15) has a satisfying intuitive interpretation associated with the effect of correlations on the density profiles shown in Fig. 1. For small Γ values the pressure p is nearly that of an ideal gas. This positive pressure causes the density profile to expand and extend beyond the cold-fluid radius, and so the shift in the value of density moments is also positive. However, for large Γ the density profile contracts within the cold-fluid surface because the pressure becomes negative, and this is also reflected in the shift to the moments given by Eq. (2.15).

In Fig. 3 we test Eq. (2.15) in the extreme case of a crystallized plasma at $\Gamma \rightarrow \infty$, comparing the prediction to numerical simulations for various plasma shapes. In the large Γ limit the internal energy is due entirely to the lattice Madelung energy, and is well approximated for several stable lattices by $U_{\text{OCP}}/NkT \approx -0.896\Gamma$ [13,14], so from Eq. (2.10) $p/(M \omega_p^2 n_0) \approx -0.0996a_{\text{WS}}^2$. The fluid dimensions R and L are, as always, determined in terms of the trap parameter β and the particle number N via Eqs. (2.6) and (2.7). We would expect that higher-order moments would not agree as well with Eq. (2.15) since as l or m increases, $z^{2l} \rho^{2m}$ varies more rapidly through the edge region and the Taylor expansion at the edge becomes less well justified. However, there is good agreement for the moments tested, even though there is no well-defined narrow boundary region in the plasma density at these large Γ values, and $n(r; \Gamma)$ is unequal to $n_f(r)$ over the entire plasma.

In Fig. 4 we test the Γ dependence of the density moments for finite temperature spherical plasma equilibria for a range of Γ values. Here we determine the plasma pressure p using the known results for $U_{\text{OCP}}(\Gamma)/NkT$ [13,14], and again there is good agreement between Eq. (2.15) and the simulations over a range of Γ values. In this case the simulations are equilibrium Monte Carlo simulations, as in Fig. 2, some with $N = 512$, others with $N = 256$.

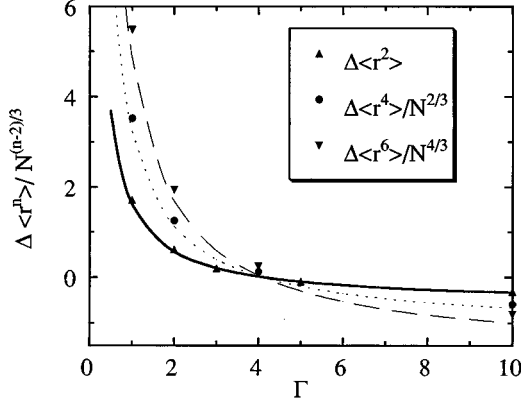


FIG. 4. Difference between simulations and cold-fluid theory for density moments $\langle r^2 \rangle$, $\langle r^4 \rangle$, and $\langle r^6 \rangle$, where r is spherical radius, as a function of correlation parameter Γ for a spherical plasma ($\alpha = \beta = 1$). Dots: Monte Carlo simulations. Lines: theoretical predictions of Eq. (2.15). Lengths are measured in units of a_{WS} .

In summary, interparticle correlations and finite temperature give rise to effects not present in the fluid equilibrium of Sec. II A, such as the formation of liquid and crystalline states. Although the detailed microscopic correlations for these states are quite complex, their effect on low-order moments of the density can be understood using a model which accounts for correlations and temperature through the bulk plasma pressure.

III. NORMAL MODES

We now turn to the electrostatic normal modes of these trapped plasmas. Both magnetized plasma and upper hybrid oscillations have been excited in recent experiments. In some experiments [1, 2, 4] the measured frequencies agree with a cold-fluid theory [6] of the modes of a uniform density plasma spheroid in a harmonic trap, but in other experiments noticeable frequency shifts were induced by the effects of finite temperature and trap anharmonicity [3]. In addition, computer simulations have observed frequency shifts for modes excited in strongly correlated plasmas [7]. Here we will derive general results for the frequency shifts of the normal modes due to correlations. In order to make contact with the experiments and with simulations, we will consider the extreme limits of very strong applied magnetic field where guiding center equations of motion apply, and zero magnetic field. In a Penning trap the magnetic field can appear to be zero in a frame rotating with the plasma. The cyclotron frequency Ω_c is shifted by rotation to the vortex frequency $\Omega_v = \Omega_c + 2\omega_r$. The plasma becomes unmagnetized in the rotating frame when $\Omega_v = 0$, which occurs at the Brillouin limit $\omega_r = -\Omega_c/2$. The unmagnetized limit also applies to modes excited in a Paul trap plasma.

A. Fluid theory

We first review the cold-fluid theory of the normal modes. In cold-fluid theory perturbations away from equilibrium are described by the linearized continuity, momentum, and Poisson equations in a frame rotating with the plasma:

$$\frac{\partial}{\partial t} \delta n + \nabla \cdot (n_f \delta \mathbf{v}) = 0, \quad (3.1a)$$

$$\frac{\partial}{\partial t} \delta \mathbf{v} = -\frac{q}{M} \nabla \psi + \Omega_v \delta \mathbf{v} \times \hat{z}, \quad (3.1b)$$

$$\nabla^2 \psi = -4\pi q \delta n, \quad (3.1c)$$

where δn , $\delta \mathbf{v}$, and ψ are perturbed density, velocity, and potential, respectively. Under the assumption that modes vary in time in the rotating frame as $\exp(-i\omega t)$, standard manipulations of Eqs. (3.1) then yield

$$\nabla \cdot (\boldsymbol{\varepsilon} \cdot \nabla \psi) = 0, \quad (3.2a)$$

where

$$\boldsymbol{\varepsilon} = \begin{pmatrix} \varepsilon_1 & -i\varepsilon_2 & 0 \\ i\varepsilon_2 & \varepsilon_1 & 0 \\ 0 & 0 & \varepsilon_3 \end{pmatrix} \quad (3.2b)$$

is the cold plasma dielectric tensor. Outside the spheroid, $\varepsilon = 1$, whereas inside,

$$\varepsilon_1 = 1 - \frac{\omega_p^2}{(\omega^2 - \Omega_v^2)}, \quad \varepsilon_2 = \frac{\omega_p^2 \Omega_v}{\omega(\omega^2 - \Omega_v^2)}, \quad \varepsilon_3 = 1 - \frac{\omega_p^2}{\omega^2}. \quad (3.2c)$$

Equation (3.2a) is Maxwell's equation $\nabla \cdot \mathbf{D} = 0$ for a medium with a frequency-dependent dielectric tensor $\boldsymbol{\varepsilon}$. Formulation of the eigenmode problem is completed by the boundary condition $\psi \rightarrow 0$ at $|\mathbf{x}| \rightarrow \infty$ (i.e., image charges in the trap walls are neglected, which is a good approximation for small plasmas and distant walls).

Unmagnetized modes

We first consider the unmagnetized limit, which is particularly simple. In this limit the modes fall into two categories: bulk plasma oscillations which produce no potential variation outside the plasma, and surface plasma oscillations which are incompressible distortions of the plasma shape, and which induce potential variations outside the plasma.

Outside the plasma $\varepsilon = 1$ and ψ satisfies Laplace's equation

$$\nabla^2 \psi^{\text{out}} = 0, \quad (3.3a)$$

whereas inside the plasma $\varepsilon_2 = 0$ and $\varepsilon_1 = \varepsilon_3$, and Eq. (3.2) becomes

$$\left(1 - \frac{\omega_p^2}{\omega^2}\right) \nabla^2 \psi^{\text{in}} = 0, \quad (3.3b)$$

so either $\omega^2 = \omega_p^2$, or else ψ^{in} also satisfies Laplace's equation. In either case the inner and outer potentials must match across the plasma surface S :

$$\psi^{\text{in}}(\mathbf{x}) = \psi^{\text{out}}(\mathbf{x})|_S, \quad (3.4a)$$

$$\left(1 - \frac{\omega_p^2}{\omega^2}\right) \hat{\mathbf{u}} \cdot \nabla \psi^{\text{in}} = \hat{\mathbf{u}} \cdot \nabla \psi^{\text{out}}|_S, \quad (3.4b)$$

where $\hat{\mathbf{u}}$ is a unit vector normal to the plasma surface.

If $\omega^2 = \omega_p^2$, Eqs. (3.3a) and (3.4b) imply that $\psi^{\text{out}} = 0$, whereas Eq. (3.3b) implies ψ^{in} is undefined. This solution corresponds to bulk plasma oscillations with an undefined density dependence δn inside the plasma. In fact, the density perturbation is not entirely undefined since Eq. (3.4) specifies ψ_{in} at the boundary; only density perturbations which produce no potential outside the plasma are allowed. For example, in a spherical plasma, any perturbation that is a function only of radius r causes no change in external potential; such modes are ‘‘breathing oscillations’’ of the cloud, and in fluid theory all such oscillations are at the plasma frequency. More complicated perturbations of this sort can also be easily constructed.

The other case, $\nabla^2 \psi^{\text{in}} = 0$, corresponds to surface plasma oscillations. The solution is separable in spheroidal coordinates (ξ_1, ξ_2, ϕ) , where [19]

$$\begin{aligned} z &= \xi_1 \xi_2, \\ \rho &= \sqrt{(\xi_1^2 - d^2)(1 - \xi_2^2)}, \end{aligned} \quad (3.5)$$

and ϕ is the usual azimuthal angle. The coordinate ξ_1 is a generalized radial coordinate, and ξ_2 is a generalized latitude. Surfaces of constant ξ_1 are confocal spheroids, and surfaces of constant ξ_2 are confocal hyperboloids everywhere normal to the constant ξ_1 surfaces. The length d is a parameter of the coordinate system, chosen as $d = \sqrt{L^2 - R^2}$ in order that the plasma surface is a constant ξ_1 surface, given by $\xi_1 = L$. The coordinate ξ_1 approaches the spherical radius r in the spherical limit $L = R$ (i.e., $d = 0$), and ξ_2 approaches $\cos\theta$ in the spherical limit. In these coordinates the solutions of Laplace’s equation inside and outside the plasma are

$$\psi^{\text{in}} = A P_l^m(\xi_1/d) P_l^m(\xi_2) \exp(im\phi), \quad (3.6a)$$

$$\psi^{\text{out}} = B Q_l^m(\xi_1/d) P_l^m(\xi_2) \exp(im\phi), \quad (3.6b)$$

where P_l^m and Q_l^m are Legendre functions, and where l and m are integer mode numbers, $l \geq |m|$, determining the spatial variation of the mode. Specifically, the number of zeros in the potential encountered upon circling the equator of the spheroid is $|m|$, whereas the number of zeros encountered upon traversing the spheroid from pole to pole along a great circle equals $l - |m|$. That these perturbations cause incompressible deformations follows from the fact that $\nabla^2 \psi = 0$ everywhere except at the plasma vacuum boundary. At the boundary the jump in the gradient of ψ corresponds to a surface charge density that can be regarded as an infinitesimal displacement of the surface.

The frequencies of these surface plasma modes are found by substitution of Eqs. (3.6) into Eqs. (3.4):

$$\omega^2 = \frac{\omega_p^2}{1 - Q_l^m P_l^m / Q_l^m P_l^m}, \quad (3.7)$$

where $Q_l^m = Q_l^m(\alpha/\sqrt{\alpha^2 - 1})$, $P_l^m = P_l^m(\alpha/\sqrt{\alpha^2 - 1})$, and the prime denotes differentiation with respect to the entire argument. In the spherical limit $\alpha = 1$ Eq. (3.7) approaches the well-known result for surface oscillations of a plasma sphere,

TABLE I. Spatial dependence of the potential ψ^{in} for the (l, m) fluid normal mode within a spheroidal plasma. Cylindrical coordinates (ρ, ϕ, z) are used. Here $\bar{d}^2 = L^2 \varepsilon_1 / \varepsilon_3 - R^2$, where R is the radius, L is the half-length of the spheroid, and the dielectric constants ε_1 and ε_3 are given in Eq. (3.2c).

(l, m)	ψ^{in}
(1,0)	z
(1,1)	$\rho e^{i\phi}$
(2,0)	$3[2z^2(\varepsilon_1/\varepsilon_3) - \rho^2]/4 - \bar{d}^2/2$
(2,1)	$\rho z e^{i\phi}$
(2,2)	$\rho^2 e^{2i\phi}$
(3,0)	$z[10z^2(\varepsilon_1/\varepsilon_3) - 15\rho^2 - 6\bar{d}^2]$
(3,1)	$\rho[20z^2(\varepsilon_1/\varepsilon_3) - 5\rho^2 - 6\bar{d}^2]e^{i\phi}$
(3,2)	$\rho^2 z e^{2i\phi}$
(3,3)	$\rho^3 e^{3i\phi}$

$$\omega^2 = \omega_p^2 l / (2l + 1). \quad (3.8)$$

Normal modes for $B \neq 0$

We now turn to the magnetized plasma oscillations of a fluid spheroid. Unlike the unmagnetized case where, for given l and m , there is a single pair of (positive and negative) surface mode frequencies satisfying Eq. (3.7), there are now several modes for a given l and m . When $m = 0$ there are l pairs of modes; when $l - m$ is odd there are $2(l - |m|) + 1$ modes, and when $l - m$ is nonzero and even there are $2(l - |m|) + 2$ modes.

The theoretical treatment of the magnetized modes is similar to that of the unmagnetized modes, and has been thoroughly discussed in previous work [1, 6]. We therefore skip directly to the relevant results. Outside the plasma Eq. (3.2) is Laplace’s equation, and so the outer solution is still Eq. (3.6b). Inside the plasma the solution is in terms of scaled spheroidal coordinates

$$\psi^{\text{in}}(\mathbf{x}) = A P_l^m(\bar{\xi}_1/\bar{d}) P_l^m(\bar{\xi}_2) \exp(im\phi), \quad (3.9)$$

where $\bar{\xi}_1$ and $\bar{\xi}_2$ are defined by the following transformation:

$$\begin{aligned} z &= \bar{\xi}_1 \bar{\xi}_2 (\varepsilon_3 / \varepsilon_1)^{1/2}, \\ \rho &= \sqrt{(\bar{\xi}_1^2 - \bar{d}^2)(1 - \bar{\xi}_2^2)}, \end{aligned} \quad (3.10)$$

where $\bar{d} = \sqrt{L^2 \varepsilon_1 / \varepsilon_3 - R^2}$. The interior potential has a relatively simple polynomial form in cylindrical coordinates. In Table I the form for ψ^{in} in cylindrical coordinates is given for values of l and m up to $(l, m) = (3, 3)$.

The eigenvalue equation equivalent to Eq. (3.7) is

$$\varepsilon_3 + m\alpha(\alpha^2 - \varepsilon_3/\varepsilon_1)^{1/2} \frac{P_l^m}{P_l^m} \varepsilon_2 = \left(\frac{\alpha^2 - \varepsilon_3/\varepsilon_1}{\alpha^2 - 1} \right)^{1/2} \frac{P_l^m Q_l^m'}{P_l^m Q_l^m}, \quad (3.11)$$

where now $P_l^m = P_l^m[\alpha/(\alpha^2 - \varepsilon_3/\varepsilon_1)^{1/2}]$, and Q_l^m has the same argument as in Eq. (3.7). It is easy to show that this

eigenvalue equation approaches Eq. (3.7) in the unmagnetized limit, where $\varepsilon_2 \rightarrow 0$ and $\varepsilon_1 \rightarrow \varepsilon_3$.

In the guiding center limit $\Omega_c \gg \omega_p \gg \omega_r$, and

$$\varepsilon_1 = 1, \quad \varepsilon_2 = -\omega_p^2/\omega\Omega_c, \quad \varepsilon_3 = 1 - \omega_p^2/\omega^2. \quad (3.12)$$

In this guiding center limit, the modes fall into three classes depending on their frequency: upper hybrid oscillations, magnetized plasma oscillations, and $\mathbf{E} \times \mathbf{B}$ drift oscillations. In the rotating frame the frequency of the upper hybrid oscillations falls in the range $|\Omega_v| < |\omega| < |\Omega_{UH}|$, where the upper hybrid frequency Ω_{UH} is $\Omega_{UH} = \sqrt{\omega_p^2 + \Omega_v^2}$. The magnetized plasma oscillations are in the range $|\omega| < \omega_p$, while the $\mathbf{E} \times \mathbf{B}$ drift modes consist of slow drift motions at low frequencies, typically $|\omega| \sim |\omega_p^2/\Omega_v|$. For example, the $l=1, m=1$ magnetron mode is an $\mathbf{E} \times \mathbf{B}$ drift motion of the center of mass about the trap axis.

Since the $\mathbf{E} \times \mathbf{B}$ modes have not been considered in much detail in previous publications on the spheroidal modes, it may be useful to make a momentary diversion to discuss their properties. The $\mathbf{E} \times \mathbf{B}$ modes exist only for $m \neq 0$ and $l - |m|$ even, in which case there is one such mode. For example, the $l=3, m=1$ $\mathbf{E} \times \mathbf{B}$ mode consists of an octopole distortion of the plasma that involves small $O(1/B)$ displacements along z as well as $O(1)$ displacements across \mathbf{B} .

The $\mathbf{E} \times \mathbf{B}$ modes may be distinguished from the magnetized plasma oscillations in that the $\mathbf{E} \times \mathbf{B}$ frequencies depend inversely on magnetic field strength in the large \mathbf{B} limit, whereas the plasma oscillations remain at finite frequency in this limit. Furthermore, in this limit the plasma oscillations involve fluid motions only along the magnetic field, whereas the $\mathbf{E} \times \mathbf{B}$ modes involve cross-field $\mathbf{E} \times \mathbf{B}$ drift motion. However, the $\mathbf{E} \times \mathbf{B}$ modes can also be thought of as low-frequency long-wavelength extensions of the magnetized plasma oscillations in that they are the modes with the longest axial wavelength for a given radial wavelength, much as diocotron modes of a cylindrical plasma column can be obtained from the long axial wavelength limit of the magnetized plasma dispersion relation.

In the large magnetic field limit an explicit solution for the $\mathbf{E} \times \mathbf{B}$ mode frequency can be extracted from Eq. (3.11). In the limit $\Omega_v \rightarrow \infty$, for the $\mathbf{E} \times \mathbf{B}$ modes $\omega \rightarrow 0$, $\varepsilon_3 \rightarrow \infty$, $\varepsilon_1 \rightarrow 1$, and $\varepsilon_2 \rightarrow \omega_p^2/\omega\Omega_v$. Then the argument of P_l^m approaches zero, and a Taylor expansion of Eq. (3.11) yields the result

$$\frac{\omega\Omega_v}{\omega_p^2} = m \left/ \left[l^2 - m^2 + l - \frac{1}{\alpha(\alpha^2 - 1)^{1/2}} Q_l^m / Q_l^{m'} \right] \right.$$

This formula generalizes a previous result [6] derived for the case of $l = |m|$ magnetron modes to include $\mathbf{E} \times \mathbf{B}$ modes for which $l \neq |m|$. For the case $l = |m|$, it is not difficult to show that $\omega\Omega_v/\omega_p^2$ is the same function of α as is ω^2/ω_p^2 for the $l = |m|$ unmagnetized surface plasma modes [Eq. (3.7)]. This is because the form of the perturbed potential is identical for both $\mathbf{E} \times \mathbf{B}$ and unmagnetized limits (see Table I).

B. Correlation effects

We now consider the effect of correlations on the low-order modes. Shifts in the mode frequencies can be accounted for through two effects which were neglected in cold-fluid theory. First, plasma pressure changes the plasma equilibrium, as was discussed in Sec. II. This change in the equilibrium shifts the frequency of the normal modes. Second, extra restoring forces appear due to pressure effects. Since we are interested here in long-wavelength (low-order) modes we model these restoring forces using bulk and shear moduli.

In addition to the frequency shift of the modes, damping can also be accounted for by allowing the bulk and shear moduli to have imaginary parts, which can be related to high-frequency bulk and shear viscosities [20]. This approach neglects thermal diffusion, anticipating that we will mainly be interested in mode damping at low temperatures (large Γ), for which such dissipative effects are typically small compared to the dissipation due to velocity shears [21].

We employ a fluid model for the plasma which includes a linear viscoelastic response to perturbations. The momentum equation, in a frame rotating with frequency ω_r , is taken to be

$$Mn \left[\frac{\partial \mathbf{v}}{\partial t} + \mathbf{v} \cdot \nabla \mathbf{v} \right] = n(-q \nabla \phi + M \Omega_v \mathbf{v} \times \hat{z}) - \nabla \cdot \pi, \quad (3.13)$$

where n is the density, \mathbf{v} the fluid velocity, ϕ the electrostatic potential as seen in the rotating frame including plasma and external fields, and π the pressure tensor that accounts for correlation effects.

We first consider equilibria of Eq. (3.13), described by an equilibrium density $n^{(0)}$, potential $\phi^{(0)}$, and velocity $v^{(0)}$. We will limit discussion to thermal equilibrium so $v^{(0)} = 0$ (we work in the rotating frame) and the density and potential are then related by setting $\partial v / \partial t = 0$ in Eq. (3.13):

$$-qn^{(0)} \nabla \phi^{(0)} - \nabla p = 0. \quad (3.14)$$

Here we have also assumed that the equilibrium stress tensor is isotropic, $\pi_{ij}^{(0)} = \delta_{ij} p$, where p is the bulk pressure. This approximation neglects surface tension effects on the equilibrium.

In the weakly correlated limit $p = n^{(0)} kT$, and if T is constant, Eq. (3.14) leads to the Boltzmann distribution for the density. However, when the plasma is strongly correlated Eq. (3.14), together with the equation of state, Eq. (2.10), is equivalent to the local density approximation of density functional theory [22]. It must be remembered that in the strongly correlated limit the equilibrium density $n^{(0)}$ which results from solution of Eq. (3.14) is only an approximation to the exact single-particle density $n(\mathbf{x}; \Gamma)$ obtained from Eq. (2.9); in fact, bounded solutions of Eq. (3.14) do not exist when $\Gamma \gg 1$. Nevertheless, we will find that the equations we obtain for the normal modes are well behaved, even though the equilibrium equations may be ill posed. This is because our theory for the low-order normal modes will only require moments of the equilibrium density, so in effect only low-order polynomial moments of Eq. (3.14) will be required. One can show that such moments can be extracted using an

analogous approach to that used in Appendix A and Sec. II; in fact, such an analysis yields a correlation correction to the moments identical to the rigorous result of Eq. (2.15). Thus low-order moments of $n^{(0)}$ are identical to moments of the exact single-particle density $n(\mathbf{x};\Gamma)$, but the detailed functional forms of $n^{(0)}$ and $n(\mathbf{x};\Gamma)$ may differ on the scale of an interparticle spacing.

This point bears repeating: the fluid equations we employ are not well posed in the strongly correlated limit, except in the sense that low-order moments of $n^{(0)}$ can be extracted from Eq. (3.14). Fortunately, we will see that our analysis requires only these low-order moments.

Linear perturbations around the equilibrium are described by subtracting Eq. (3.14) from Eq. (3.13),

$$Mn^{(0)}\frac{\partial\delta\mathbf{v}}{\partial t}=n^{(0)}[-q\nabla\delta\phi+M\Omega_v\delta\mathbf{v}\times\hat{z}] -q\delta n\nabla\phi^{(0)}-\nabla\cdot\delta\pi, \quad (3.15)$$

where $\delta\pi$ is the change in the pressure tensor, $\delta\phi$ is the perturbed potential, and δn and $\delta\mathbf{v}$ are the perturbed density and fluid velocity, respectively. We employ the notation $\delta\phi$ for the perturbed potential in order to distinguish it from the cold-fluid theory limit ψ of Sec. III A. The perturbed pressure can be separated into pressure changes at a point due to convection, and pressure changes due to strains in the plasma:

$$\delta\pi_{ij}=-\delta\mathbf{x}\cdot\nabla p\delta_{ij}-s_{ij}, \quad (3.16)$$

where $\delta\mathbf{x}$ is the change in position of a fluid element from equilibrium, related to $\delta\mathbf{v}$ through $\delta\mathbf{v}=d\delta\mathbf{x}/dt$. We employ a viscoelastic approximation for the stress tensor s_{ij} useful for long-wavelength perturbations [20]:

$$s_{ij}=\eta_{ijkl}u_{kl}, \quad (3.17)$$

where η_{ijkl} depends on bulk and shear moduli, and the strain tensor u_{ij} is given in terms of the displacement $\delta\mathbf{x}$ of a fluid element,

$$u_{ij}=\frac{1}{2}\left(\frac{\partial\delta x_i}{\partial x_j}+\frac{\partial\delta x_j}{\partial x_i}\right). \quad (3.18)$$

For example, for an unmagnetized plasma (a Paul trap plasma or a Penning trap plasma at the Brillouin limit),

$$s_{ij}=\kappa u_{ll}\delta_{ij}+2\mu[u_{ij}-\frac{1}{3}u_{ll}\delta_{ij}], \quad (3.19a)$$

where κ and μ are the bulk and shear modulus, respectively.

This form of the perturbed pressure tensor assumes an isotropic medium, which is certainly not true for a perfect crystal in which bulk and shear moduli typically depend on the direction of strain with respect to the crystal axes. However, in the systems considered here the crystalline symmetry is imperfect [15], and an approach based on a model of the plasma as an isotropic amorphous material is useful.

The addition of a magnetic field also affects the relationship between stress and strain in an amorphous material. Symmetry considerations imply that the two moduli of Eq. (3.19a) must in general be replaced by seven moduli: two bulk moduli κ and κ_1 , and five shear moduli, μ ,

$\mu_1 \dots \mu_4$ [23]. Taking the magnetic field to be in the z direction, the stress tensor takes the form

$$\begin{aligned} s_{xx} &= \kappa\nabla\cdot\delta\mathbf{x} + \kappa_1 u_{zz} + 2\mu(u_{xx} - \frac{1}{3}\nabla\cdot\delta\mathbf{x}) + \mu_1(u_{xx} - u_{yy}) \\ &\quad + 2\eta_3 v_{xy}, \\ s_{yy} &= \kappa\nabla\cdot\delta\mathbf{x} + \kappa_1 u_{zz} + 2\mu(u_{yy} - \frac{1}{3}\nabla\cdot\delta\mathbf{x}) - \mu_1(u_{xx} - u_{yy}) \\ &\quad - 2\eta_3 v_{xy}, \\ s_{zz} &= (\kappa + \kappa_1)\nabla\cdot\delta\mathbf{x} + \kappa_1 u_{zz} + 2\mu(u_{zz} - \frac{1}{3}\nabla\cdot\delta\mathbf{x}), \\ s_{xy} &= s_{yx} = 2(\mu + \mu_1)u_{xy} - \eta_3(v_{xx} - v_{yy}), \\ s_{xz} &= s_{zx} = 2(\mu + \mu_2)u_{xz} + 2\eta_4 v_{yz}, \\ s_{yz} &= s_{zy} = 2(\mu + \mu_2)u_{yz} - 2\eta_4 v_{xz}, \end{aligned} \quad (3.19b)$$

where v_{ij} is the symmetrized velocity strain tensor, $v_{ij}=du_{ij}/dt$, and in order to deal with strictly real coefficients in the nondissipative limit we have replaced μ_3 and μ_4 by shear viscosities η_3 and η_4 . For an oscillating strain at frequency ω these coefficients are related by $\mu_{3(4)}=-i\omega\eta_{3(4)}$. It is important to note that the real parts of the viscosities η_3 and η_4 do not give rise to dissipation as the stress they create is perpendicular to the flow; these terms arise through the Lorentz force $\mathbf{v}\times\mathbf{B}$. In fact, even in the limit of a collisionless magnetized plasma, where there is no dissipation, these two coefficients are nonzero due to finite Larmor radius effects [23].

In principle all seven moduli are required when the vortex frequency Ω_v is nonzero, but some simplifications are possible in certain limits. For $\Gamma\gg 1$ the plasma is crystallized, and dissipative contributions to the moduli (the imaginary parts) are small and may sometimes be neglected. Furthermore the nondissipative contributions, which describe the restoring forces in the crystal lattice due to applied strains, depend only on static properties of the equilibrium. Since static properties of the classical crystal are independent of the magnetic field, the unmagnetized limit of the stress tensor, Eq. (3.19a), again applies for crystallized plasmas.

The linearized momentum equation, Eq. (3.15), together with linearized continuity and Poisson equations

$$\delta n + \nabla\cdot n^{(0)}\delta\mathbf{x}=0, \quad (3.20)$$

$$\nabla^2\delta\phi=-4\pi q\delta n \quad (3.21)$$

are a closed set of five homogeneous partial differential equations for the five independent scalar functions given by δn , $\delta\phi$, and $\delta\mathbf{x}$. These equations, together with the boundary condition $\delta\phi\rightarrow 0$ as $|\mathbf{x}|\rightarrow\infty$, constitute an eigenvalue problem for the normal modes.

We do not attempt an exact solution of this complex problem, except for a special case discussed in Appendix B. Instead, we employ an approach based on perturbation theory around the known solutions for an uncorrelated uniform plasma spheroid. This approach will be sufficient to obtain the lowest-order corrections to the mode frequency due to strong correlation effects.

We first construct an equation for the perturbed potential similar to the cold-fluid equation, Eq. (3.2a). With the help of Eq. (3.14) we rewrite Eq. (3.15) as

$$\delta\mathbf{x} = \frac{\sigma}{4\pi q n_0} \cdot \left[\nabla \delta\phi - \frac{\delta n \nabla p}{q n^{(0)2}} + \frac{\nabla \cdot \delta\pi}{q n^{(0)}} \right], \quad (3.22)$$

where σ is a scaled conductivity tensor. Its components in Cartesian coordinates are

$$\sigma = \begin{pmatrix} \sigma_1 & i\sigma_2 & 0 \\ -i\sigma_2 & \sigma_1 & 0 \\ 0 & 0 & \sigma_3 \end{pmatrix},$$

where

$$\begin{aligned} \sigma_1 &= \omega_p^2 / (\omega^2 - \Omega_v^2), & \sigma_2 &= \omega_p^2 \Omega_v / \omega (\omega^2 - \Omega_v^2) \\ \text{and } \sigma_3 &= \omega_p^2 / \omega^2. \end{aligned} \quad (3.23)$$

Substitution of Eq. (3.22) into Eqs. (3.20) and (3.21) then leads to the following equation for the perturbed potential:

$$\nabla^2 \delta\phi - \nabla \cdot \sigma \frac{n^{(0)}}{n_0} \cdot \left[\nabla \delta\phi + \nabla^2 \delta\phi \frac{\nabla p}{4\pi q^2 n^{(0)2}} + \frac{\nabla \cdot \delta\pi}{q n^{(0)}} \right] = 0. \quad (3.24)$$

In perturbation theory we break Eq. (3.24) into a zeroth order part and a correction

$$\hat{L}(\omega) \delta\phi = \hat{C} \delta\phi, \quad (3.25)$$

where $\hat{L}(\omega)$ is a frequency dependent linear operator corresponding to the cold-fluid eigenmode equation

$$\hat{L}(\omega) \delta\phi \equiv \nabla \cdot (\varepsilon \cdot \nabla \delta\phi), \quad (3.26)$$

and the cold-fluid dielectric tensor ε is given by Eq. (3.2b). The equation $\hat{L} \delta\phi = 0$, $\delta\phi \rightarrow 0$ at $|\mathbf{x}| \rightarrow \infty$ leads to the dispersion relation of Eq. (3.11). The correction $\hat{C} \delta\phi$ to this equation causes frequency shifts. It can be written as

$$\hat{C} \delta\phi = \nabla \cdot \sigma \cdot \left\{ \Delta \bar{n} \nabla \delta\phi + \frac{\nabla^2 \delta\phi \nabla p}{M n^{(0)} \omega_p^2} + \frac{\nabla \cdot \delta\pi}{q n_0} \right\}, \quad (3.27)$$

where $\Delta \bar{n} \equiv [n^{(0)}(\mathbf{x}) - n_f(\mathbf{x})] / n_0$ is the difference between the correlated equilibrium density $n^{(0)}$ and the cold-fluid density n_f , scaled by the background density n_0 . This difference is negligible by assumption except near the surface of the plasma.

The operator \hat{L} is Hermitian with respect to the norm $(f, g) = \int d^3x f^* g$, and so a standard first-order perturbation approach can be employed. One writes the solution to Eq. (3.25) as $\delta\phi = \psi + \Delta\psi$, where ψ is a solution to the cold-fluid eigenvalue problem $\hat{L}(\omega_f) \psi = 0$ for some fluid mode frequency ω_f . The solution is given explicitly by Eqs. (3.6b), (3.9), and (3.11).

The eigenmode frequency ω also shifts slightly, to $\omega = \omega_f + \Delta\omega$. By keeping corrections only to first order in the perturbed quantities in Eq. (3.25), one obtains

$$\Delta\omega \frac{\partial \hat{L}}{\partial \omega_f} \psi + \hat{L}(\omega_f) \Delta\psi = \hat{C} \psi. \quad (3.28)$$

The frequency shift $\Delta\omega$ can then be extracted by taking the inner product of this equation with ψ . Since \hat{L} is Hermitian, $(\psi, \hat{L} \Delta\psi) = (\Delta\psi, \hat{L} \psi)^* = 0$, and so the frequency shift satisfies

$$\Delta\omega = \frac{(\psi, \hat{C} \psi)}{\left(\psi, \frac{\partial \hat{L}}{\partial \omega_f} \psi \right)}. \quad (3.29)$$

In order for this perturbation approach to be valid, $\Delta\psi$ must be small compared to ψ [24]. This constrains the sorts of perturbations one can consider. For example, in Eq. (3.27) let us arbitrarily neglect all terms except for the first, $\nabla \cdot \sigma \Delta \bar{n} \cdot \nabla \delta\phi$. One might imagine a perturbation of a given cold-fluid equilibrium which consists of a slight change in shape of the spheroid to another cold-fluid equilibrium; then only this term would be nonzero. Furthermore, the frequency shift could then be determined exactly by using the exact eigenmode equation, Eq. (3.11), for the two spheroidal equilibria. However, one can easily check that the result from perturbation theory, Eq. (3.29) does *not* provide the right answer in this case. This is because the function $\Delta \bar{n}$ is of $O(1)$ at the plasma edge, and varies rapidly. Such perturbations are not small, even though the width of the region over which $\Delta \bar{n}$ is large may be small. Since the change in $\Delta \bar{n}$ is both large and abrupt in this example, $\Delta\psi$ turns out to be the same order of magnitude as ψ .

It is not obvious that the more physical case of perturbations to the modes due to pressure shifts in the density profile will not also lead to a breakdown of the perturbation theory. However, in Appendix B we show that for such pressure shifts the perturbed eigenfunction $\Delta\psi$ is in fact small compared to ψ .

As an example, we evaluate $\Delta\psi$ for the case of a (2,0) mode in an unmagnetized spherical plasma. As discussed in Appendix B, $\Delta\psi$ for this mode has the form

$$\Delta\psi = \frac{\delta\mathbf{x} \cdot \nabla p}{q n_0} + \frac{\mu + 2p/5}{M n_0 \omega_p^2 R^2} \psi(R, \theta) f(r), \quad (3.30)$$

where spherical coordinates (r, θ, ϕ) are used, $\psi(R, \theta)$ is the (2,0) cold-fluid mode potential evaluated at the surface of the plasma (see Table I for the form of this potential in cylindrical coordinates), and $f(r)$ is a dimensionless function displayed in Fig. 5. The discontinuity in $f(r)$ at the edge of the plasma is due to a boundary layer that forms when damped bulk plasma oscillations are coupled to the (2,0) surface mode by correlation effects.

We also compare our expressions for the frequency shift and eigenfunctions to a known exact solution of Eqs. (3.15), (3.20), and (3.21) for an unmagnetized spherical plasma. Our perturbation results match the exact results in this case. The interested reader is referred to Appendix B for the details.

The inner products in Eq. (3.29) may be written in terms of polynomial moments of the thermal equilibrium density, determined by Eqs. (2.8) and (2.15). This is a great simplification since all inner products of Eq. (3.29) can then be

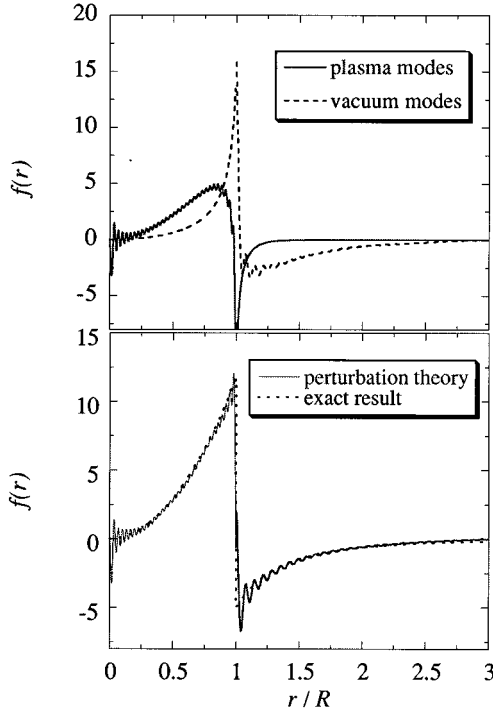


FIG. 5. Normalized perturbed potential eigenfunction $f(r)$ for the (2,0) mode in a spherical unmagnetized plasma of radius R [see Eq. (3.30), or Eqs. (B9) and (B10)]. The upper figure shows the plasma and vacuum contributions to f arising from the perturbation analysis of Appendix B, keeping the first 62 plasma eigenfunctions and the first 57 vacuum eigenfunctions. The lower figure compares f from perturbation theory (solid) to the exact solution in the limit $R/a_{\text{WS}} \gg 1$, Eq. (B25) (dotted).

determined analytically. Since the numerator of Eq. (3.29) is small by assumption, the denominator need be evaluated only to lowest order, which implies that the fluid density $n_f(\mathbf{x})$ may be used when evaluating $\partial \hat{L} / \partial \omega$. Integration by parts then leads to the expression

$$\begin{aligned} \left(\psi, \frac{\partial \hat{L}}{\partial \omega} \psi \right) &= \int_{\text{in}} d^3x \nabla \psi^{\text{in}*} \cdot \frac{\partial \sigma}{\partial \omega} \cdot \nabla \psi^{\text{in}} \\ &= - \int_{\text{in}} d^3x \left[\alpha_1 \left(\left| \frac{\partial \psi^{\text{in}}}{\partial \rho} \right|^2 + \frac{m^2}{\rho^2} |\psi^{\text{in}}|^2 \right) \right. \\ &\quad \left. - \frac{2m\alpha_2 \psi^{\text{in}}}{\rho} \frac{\partial \psi^{\text{in}*}}{\partial \rho} + \alpha_3 \left| \frac{\partial \psi^{\text{in}}}{\partial z} \right|^2 \right], \end{aligned} \quad (3.31)$$

where

$$\begin{aligned} \alpha_1 &= 2\omega\omega_p^2/(\omega^2 - \Omega_v^2)^2, \\ \alpha_2 &= \Omega_v\omega_p^2(3\omega^2 - \Omega_v^2)/\omega^2(\omega^2 - \Omega_v^2)^2 \\ \text{and } \alpha_3 &= 2\omega_p^2/\omega^3, \end{aligned} \quad (3.32)$$

and the integral is over the interior of the fluid spheroid. Since the cold-fluid potential ψ^{in} can be written as a polyno-

mial in ρ and z (see Table I), and $\alpha_1 \dots \alpha_3$ are constants, the integral in Eq. (3.31) can be evaluated in terms of fluid moments given by Eq. (2.8).

The numerator of Eq. (3.29) can also be written in terms of fluid density moments as well as the correlation corrections to these moments, as given by Eqs. (2.8) and (2.14). Using Eq. (3.27), integration by parts yields

$$\begin{aligned} (\psi, \hat{C} \psi) &= - \int d^3x \left[\Delta \bar{n} \nabla \psi^* \cdot \sigma \cdot \nabla \psi + \nabla^2 \psi \frac{\delta \mathbf{x}_f^* \cdot \nabla p}{qn^{(0)}} \right. \\ &\quad \left. + 4\pi \delta \mathbf{x}_f^* \cdot \nabla \cdot \delta \pi \right], \end{aligned} \quad (3.33)$$

where

$$\delta \mathbf{x}_f \equiv \sigma \cdot \frac{\nabla \psi}{4\pi q n_0} \quad (3.34)$$

is the fluid-theory change in position of a fluid element [this follows by neglecting pressure corrections in Eq. (3.22) or, alternatively, from Eq. (3.1b)].

In order to make further progress we must now make several approximations to Eq. (3.33) based on the strongly correlated limit. In this limit $\Delta \bar{n}$, p , and $\delta \pi$ are nonzero only within the region bounded by the surface of the fluid spheroid, since the plasma contracts within this surface; see Fig. 1. We may therefore replace ψ by ψ^{in} in Eq. (3.33). Furthermore, in the second term of Eq. (3.33) we note that ∇p is already a correlation correction, so we replace the correlated density $n^{(0)}$ by the fluid density n_f . This approximation cannot be rigorously justified unless $\Delta \bar{n} \ll 1$ wherever ∇p is nonzero. We therefore assume this ordering, although it does not appear to hold for the actual equilibrium profiles (see Fig. 1).

Although taking $\Delta \bar{n} \ll 1$ appears to be a poor assumption, there are several indications that it is actually a good approximation. First and foremost, we will find that the results generated by this approximation match the known exact results for the effects of correlations on the modes. In a following paper [7], we will also show that the results for correlation frequency shifts match numerical simulations of the modes in strongly correlated plasmas. Furthermore there is some theoretical justification for this approximation: we have already observed in Sec. II that the exact equilibrium density $n(\mathbf{x}; \Gamma)$ is nearly the same as the cold-fluid density $n_f(\mathbf{x})$ in the sense that low-order moments of the two densities are nearly identical. We also observed in connection with Eq. (3.14) that in the strongly correlated limit our fluid equations for $n^{(0)}(\mathbf{x})$ cannot reproduce the exact functional form of $n(\mathbf{x}; \Gamma)$; only low-order moments of $n^{(0)}$ match those of $n(\mathbf{x}; \Gamma)$. One might, therefore, interpret $n^{(0)}$ as a coarse-grained version of $n(\mathbf{x}; \Gamma)$, with identical low-order moments but with a different functional form that nearly matches $n_f(\mathbf{x})$, so that $\Delta \bar{n} \ll 1$ is satisfied. The coarse-grained density $n^{(0)}$ does not have the correct form on the scale of an interparticle spacing, but we do not expect an approach based on fluid equations to work on such a scale. In fact, we will find that when we assume $\Delta \bar{n} \ll 1$ our results for the frequency shifts depend on $n^{(0)}$ only through low-order moments, so the interpretation of $n^{(0)}$ as a smooth coarse-

grained version of $n(r; \Gamma)$ is consistent in the sense that our results do not depend on the detailed variations of $n^{(0)}$ on the scale of an interparticle spacing. Nevertheless, while these arguments are somewhat persuasive, they are certainly not rigorous. A rigorous justification of the assumption $\Delta \bar{n} \ll 1$, or a better approach in which this assumption need not be made, remains an outstanding problem.

In any case, we then integrate by parts once on the second term of Eq. (3.33) and twice on the third, substituting Eq. (3.16) for $\delta\pi$, and we neglect the surface integrals since by assumption p and s_{ij} are zero at the surface of the fluid spheroid (the strongly correlated plasma has shrunk within this boundary surface). The result is

$$(\psi, \hat{C}\psi) = - \int d^3x \{ \Delta \bar{n} \nabla \psi^{\text{in}*} \cdot \sigma \cdot \nabla \psi^{\text{in}} - 4\pi p [\nabla \cdot (\delta \mathbf{x}_f^* u_{ii}) + \nabla \cdot (\delta \mathbf{x}_f u_{ii}^*)] + 4\pi u_{ij}^* s_{ij} \}, \quad (3.35)$$

where the Einstein summation convention is employed.

According to Eq. (3.29), division of Eq. (3.35) by Eq. (3.31) yields a general result for the frequency shift due to correlations:

$$\Delta \omega = - \left\{ 4\pi p \left[\left\langle \nabla^2 \left(\frac{\nabla \psi^{\text{in}*}}{4\pi q n_0} \cdot \delta \mathbf{x}_f \right) \right\rangle_f - 2 \langle \text{Re} [\nabla \cdot (\delta \mathbf{x}_f^* \nabla \cdot \delta \mathbf{x}_f)] \rangle_f \right] + 4\pi \eta_{ijkl} \langle u_{ij}^* u_{kl} \rangle_f \right\} / \left\langle \nabla \psi^{\text{in}*} \cdot \frac{\partial \sigma}{\partial \omega} \cdot \nabla \psi^{\text{in}} \right\rangle_f. \quad (3.36)$$

Here we have employed Eqs. (2.14) and (3.17), and the notation $\langle \rangle_f$ refers to an average over the cold-fluid density. The strain tensor u_{ij} is determined by the cold-fluid displacement $\delta \mathbf{x}_f$ through Eq. (3.18), and $\delta \mathbf{x}_f$ is determined by the cold-fluid potential ψ^{in} through Eq. (3.34). Since $\psi^{\text{in}}(\mathbf{x})$ can be written as a polynomial in ρ and z (see Table I), the averages in Eq. (3.36) can be explicitly evaluated using Eq. (2.8).

The general expression can be simplified in the unmagnetized limit. In this case the surface plasma modes are incompressible so $u_{ii} = \nabla \cdot \delta \mathbf{x}_f = 0$. Furthermore $\alpha_2 = \sigma_2 = 0$, $\sigma_1 = \sigma_3$, $\alpha_1 = \alpha_3 = 2\sigma_3/\omega$, and the isotropic form for the stress tensor, Eq. (3.19a), can be employed. Equation (3.36) then reduces to

$$\Delta \omega = \frac{\omega}{2} \frac{\frac{p}{M n_0 \omega_p^2} \langle \nabla^2 |\nabla \psi^{\text{in}}|^2 \rangle_f + \frac{2\mu}{M n_0 \omega^2} \sum_{ij} \langle |\partial^2 \psi^{\text{in}} / \partial x_i \partial x_j|^2 \rangle_f}{\langle |\nabla \psi^{\text{in}}|^2 \rangle_f} \quad (\text{unmagnetized}), \quad (3.37)$$

where ω is the frequency of the cold-fluid surface mode given by Eq. (3.7).

The term in Eq. (3.37) involving the equilibrium pressure p describes the effect on the mode frequencies of the change in the plasma equilibrium caused by pressure. The bulk modulus κ does not appear in Eq. (3.37) because the surface plasma modes are incompressible. The positive shear modulus μ increases the frequency of all modes, as one would expect since the shear modulus adds an extra restoring force.

The expression for the frequency shift also simplifies in the limit of large magnetic fields, $\Omega_v \rightarrow \infty$. We limit consideration to magnetized plasma oscillations, for which the perturbed fluid displacement $\delta \mathbf{x}$ is parallel to $\hat{\mathbf{z}}$ due to the strong magnetic field, and mode frequencies are on the order of the plasma frequency ω_p . In this case σ_1 , σ_2 , α_1 , and α_2 all are negligible [see Eqs. (3.23) and (3.32)], the magnetized form of the stress tensor, Eq. (3.19b), must be used, and the frequency shift for magnetized plasma oscillations is

$$\Delta \omega = \frac{\omega}{2} \left\{ \frac{p}{M n_0 \omega_p^2} \left\langle \nabla^2 \left| \frac{\partial \psi^{\text{in}}}{\partial z} \right|^2 \right\rangle_f - \frac{p}{M n_0 \omega^2} \left\langle \frac{\partial^2}{\partial z^2} \left| \frac{\partial \psi^{\text{in}}}{\partial z} \right|^2 \right\rangle_f + \frac{(\kappa + 2\kappa_1 + \frac{4}{3}\mu)}{M n_0 \omega^2} \left\langle \left| \frac{\partial^2 \psi^{\text{in}}}{\partial z^2} \right|^2 \right\rangle_f + \frac{(\mu + \mu_2)}{M n_0 \omega^2} \left\langle \left| \frac{\partial^2 \psi^{\text{in}}}{\partial x \partial z} \right|^2 + \left| \frac{\partial^2 \psi^{\text{in}}}{\partial y \partial z} \right|^2 \right\rangle_f + \frac{2\eta_4}{M n_0 \omega} \left\langle \frac{\partial^2 \psi^{\text{in}*}}{\partial x \partial z} \frac{\partial^2 \psi^{\text{in}}}{\partial y \partial z} \right\rangle_f \right\} / \left\langle \left| \frac{\partial \psi^{\text{in}}}{\partial z} \right|^2 \right\rangle_f. \quad (3.38)$$

Each low-order mode can also be considered on a case-by-case basis. For example, for the (1,0) and (1,1) modes, ψ^{in} is linear in ρ and z which implies that $\delta \mathbf{x}_f$ is constant and u_{ij} is zero, so $(\psi, \hat{C}\psi) = 0$ and there is no frequency shift for the (1,0) or (1,1) modes, as expected for these center of mass modes. This is an important check on the validity of our results.

A nontrivial frequency shift first appears for the (2,0) mode. Using the result for ψ^{in} from Table I in Eq. (3.36), we find that the (2,0) frequency is shifted by

$$\Delta \omega_{20} = 10 \frac{p(\sigma_1 \varepsilon_3^2 + 2\sigma_3 \varepsilon_1^2) + (\kappa - 2p)(\sigma_1 - \sigma_3)^2 - 2\kappa_1 \varepsilon_1 \sigma_3 (\sigma_1 - \sigma_3) + \mu(\varepsilon_3 \sigma_1 + 2\varepsilon_1 \sigma_3)^2 / 3}{M \omega_p^2 n_0 [\alpha_1 (\varepsilon_3 R)^2 + 2\alpha_3 (\varepsilon_1 L)^2]}, \quad (3.39)$$

where ε_i , σ_i , and α_i ($i=1, 2$, and 3) are given by Eqs. (3.2c), (3.23), and (3.32), respectively. As was previously discussed, there are two (2,0) modes, an upper hybrid mode and a plasma mode. Equation (3.39) provides the shift for both modes. In the guiding center limit $\sigma_1 \rightarrow 0$, $\alpha_1 \rightarrow 0$, and $\varepsilon_1 \rightarrow 1$, so the shift for the (2,0) plasma mode is

$$\Delta\omega_{20} = \frac{5\omega}{2L^2} \frac{2p\varepsilon_3 + (\kappa + 2\kappa_1 + 4\mu/3)\sigma_3}{M\omega_p^2 n_0}, \quad (3.40)$$

a result which also follows from Eq. (3.38). A measurement of the (2,0) frequency shift therefore provides information on the modulus of compressibility along \mathbf{B} , $\kappa + 2\kappa_1 + 4\mu/3$.

In Refs. [3] and [25] a similar (but not identical) form for the frequency shift of the magnetized (2,0) mode is derived using a different method. The difference arises because thermal equilibrium was assumed to occur only along a field line in Refs. [3] and [25], whereas true thermal equilibrium is assumed in Eq. (3.40). The results of our method and that of Refs. [3] and [25] can be shown to agree if a true thermal equilibrium is assumed in Refs. [3] and [25]. This provides another consistency check on the results.

In the unmagnetized limit $\sigma_1 = \sigma_3$ and $\alpha_1 = \alpha_3 = 2\sigma_3/\omega$ [see Eqs. (3.23) and (3.32)], so Eq. (3.39) implies a shift to the (2,0) surface plasma mode given by

$$\Delta\omega_{20} = \frac{15\omega}{R^2 + 2L^2} \frac{p + \mu\sigma_3}{M\omega_p^2 n_0}, \quad (3.41)$$

a result which could also be obtained directly from Eq. (3.37).

For the (2,1) mode, a similar analysis yields

$$\Delta\omega_{21} = 5 \frac{2(\sigma_1 - \sigma_2 + \sigma_3)p + (\sigma_1 - \sigma_2 + \sigma_3)^2(\mu + \mu_2 + \omega\eta_4)}{M\omega_p^2 n_0 [\alpha_3 R^2 + (\alpha_1 - \alpha_2)/L^2]}. \quad (3.42)$$

In the strongly magnetized guiding center limit the (2,1) frequency correction becomes

$$\Delta\omega_{21} = \frac{5}{2} \frac{\omega}{R^2} \frac{2p + (\mu + \mu_2 + \omega\eta_4)\sigma_3}{M\omega_p^2 n_0}. \quad (3.43)$$

In the unmagnetized limit μ_2 and η_4 are zero, and Eq. (3.42) implies

$$\Delta\omega_{21} = 10 \frac{\omega}{L^2 + R^2} \frac{p + \mu\sigma_3}{M\omega_p^2 n_0}, \quad (3.44)$$

the correction to the surface plasma mode frequency. For the (2,2) mode, the general expression for the frequency shift is

$$\Delta\omega_{22} = 10 \frac{\sigma_1 - \sigma_2}{\alpha_1 - \alpha_2} \frac{p + (\sigma_1 - \sigma_2)(\mu + \mu_1 + \omega\eta_3)}{M\omega_p^2 n_0 R^2}. \quad (3.45)$$

The guiding center limit for this mode is only slightly less straightforward than for the previous modes. This is a diocotron (or $\mathbf{E} \times \mathbf{B}$ drift) mode for which the mode frequency approaches zero in the limit $\Omega_v \rightarrow \infty$. While we may still take $\sigma_1 \rightarrow 0$ and $\alpha_1 \rightarrow 0$, now σ_2 and α_2 approach finite values in the limit, and the frequency shift becomes

$$\Delta\omega_{22} = \frac{10\omega}{R^2} \frac{p - (\mu + \mu_1 + \omega\eta_3)\sigma_2}{Mn_0\omega_p^2}. \quad (3.46)$$

Note that ω is of order ω_z^2/Ω_v , and so $\sigma_2 \rightarrow -\omega_p^2/\omega\Omega_v$, and is finite in the limit as $\Omega_v \rightarrow \infty$.

In the unmagnetized limit the frequency shift is

$$\Delta\omega_{22} = \frac{5\omega}{R^2} \frac{p + \mu\sigma_3}{Mn_0\omega_p^2}. \quad (3.47)$$

Finally, for the (3,0) mode, multipole moments such as $\langle \rho^2 z^2 \rangle_f$ are required in Eq. (3.36). After substitution for these moments using Eqs. (2.8) and (2.15), the frequency shift is found to be a somewhat complicated function of the plasma properties:

$$\begin{aligned} \Delta\omega_{30} = & 70\{2p[L^2((\varepsilon_3/\varepsilon_1)^2\sigma_1 + 2\sigma_3 - 2[(\sigma_3 - \sigma_1)/\varepsilon_1]^2) + (R\varepsilon_3/\varepsilon_1)^2(\sigma_1 + \sigma_3) + 2\kappa_1 L^2\sigma_3(\sigma_3 - \sigma_1)/\varepsilon_1 \\ & + 2(\kappa + 4/3\mu)L^2[(\sigma_3 - \sigma_1)/\varepsilon_1]^2 + \mu(\varepsilon_3/\varepsilon_1)[2L^2(4\sigma_1\sigma_3 - (\varepsilon_3/\varepsilon_1)\sigma_1^2) + R^2(\varepsilon_3/\varepsilon_1)[(\sigma_1 + \sigma_3)^2 + \sigma_2^2]] \\ & + \mu_2(R\varepsilon_3/\varepsilon_1)^2[(\sigma_1 + \sigma_3)^2 + \sigma_2^2] - 2\eta_4\omega(R\varepsilon_3/\varepsilon_1)^2\sigma_2(\sigma_1 + \sigma_3)\}/Mn_0\omega_p^2\{\alpha_3[8L^4 + 4(\varepsilon_3/\varepsilon_1)R^2L^2 \\ & + 3(\varepsilon_3/\varepsilon_1)^2R^4] + 10\alpha_1(\varepsilon_3/\varepsilon_1)^2L^2R^2\}. \end{aligned} \quad (3.48)$$

This equation provides the frequency shift for the three (3,0) modes, one of which is an upper hybrid mode. The other two modes are magnetized plasma oscillations. In the guiding center limit, the frequency shift for the two (3,0) plasma oscillations reduces to

$$\Delta\omega_{30} = 35\omega \frac{2L^2[2p\varepsilon_3 + (\kappa + 2\kappa_1 + 4\mu/3)\sigma_3] + (R\varepsilon_3)^2[2p + (\mu + \mu_2)\sigma_3]}{Mn_0\omega_p^2[8L^4 + 4R^2L^2\varepsilon_3 + 3R^4\varepsilon_3^2]}. \quad (3.49)$$

Equation (3.49) provides the frequency shift for both (3,0) plasma modes, depending on which of the two fluid mode frequencies one uses in the equation.

In the unmagnetized limit, there is only one (3,0) surface plasma mode, and the correlation frequency shift is

$$\Delta\omega_{30} = \frac{70\omega(3L^2 + 2R^2)}{(2L^2 + 3R^2)(4L^2 + R^2)} \frac{(p + \mu\sigma_3)}{Mn_0\omega_p^2}. \quad (3.50)$$

The frequency shifts of Eqs. (3.36)–(3.50) have several common features. In each case a term involving the pressure p determines the effect on the mode frequency of a change in the equilibrium plasma when pressure is taken into account. Also appearing are terms involving the bulk and shear moduli which describe frequency shifts due to the elastic properties of the correlated plasma. Furthermore, in all cases the frequency shift scales as $1/(\text{plasma dimension})^2$. This is because the low-order modes have an effective wave number k on the order of the $(\text{plasma dimension})^{-1}$, and we expect from dimensional considerations that pressure corrections will enter the dispersion relation at order k^2 , as in the Bohm-Gross dispersion relation for warm plasma waves, $\omega^2 = \omega_p^2 + k^2\gamma p/Mn_0$, where γ is the ratio of specific heats [26].

Bulk plasma modes

The perturbation theory used in deriving Eq. (3.36) assumed that the fluid eigenmodes are not degenerate. However, as discussed in Sec. III A, in the unmagnetized cold-fluid limit there is a set of bulk plasma modes which are degenerate, with frequency $\omega = \omega_p$. In order to determine the effect of finite pressure on these modes the formalism of degenerate perturbation theory must be employed in the analysis. Let ψ_m be a set of normalized functions which satisfy $\hat{L}(\omega_p)\psi_m = 0$, where $\hat{L}(\omega)$ is the cold-fluid mode operator of Eq. (3.26). We construct the solution to Eq. (3.24) in terms of this set, which is assumed to span the set of degenerate solutions:

$$\delta\phi = \sum_m a_m \psi_m. \quad (3.51)$$

Writing $\omega = \omega_p + \Delta\omega$, we expand Eq. (3.24) to first order in $\Delta\omega$:

$$(\psi_n, \hat{C}\psi_m)|_{\omega=\omega_p} = -\frac{nm}{Mn_0\omega_p^2} \left[-12p + 3 \frac{\kappa(m+1)(n+1) + \frac{4}{3}\mu(m-2)(n-2)}{m+n-1} \right] R^{n+m-4} V.$$

In this expression we have used Eqs. (3.27), together with Eqs. (2.8) and (2.14), for moments of the equilibrium density.

By substituting these matrix elements in Eq. (3.52) an approximate set of eigenfunctions can be constructed by truncating the infinite sum, taking the determinant of the finite matrix, and solving the resulting polynomial equation for $\Delta\omega$. This numerical evaluation requires that we choose

$$\sum_m \left(\Delta\omega \frac{\partial \hat{L}}{\partial \omega} - \hat{C} \right) a_m \psi_m |_{\omega=\omega_p} = 0.$$

Taking the inner product of this equation with ψ_n , one finds that the vector $\{a_m\}$ must be in the nullspace of a matrix which depends on $\Delta\omega$:

$$\sum_m (\psi_n, [\Delta\omega \partial \hat{L} / \partial \omega - \hat{C}] \psi_m) a_m = 0. \quad (3.52)$$

The inner product in Eq. (3.52) can be evaluated using the moment technique in a manner analogous to the method used to evaluate Eqs. (3.31) and (3.35). An equation for $\Delta\omega$ can then be obtained by setting the determinant of the matrix in Eq. (3.52) equal to zero. For each solution of this equation for $\Delta\omega$ there is a corresponding vector $\{a_m\}$ which satisfies Eq. (3.52), and which provides us with the perturbed eigenfunction $\delta\phi$ via Eq. (3.51).

We will consider only one example of this procedure in any detail. For the case of an unmagnetized spherical plasma, there are degenerate bulk plasma modes with arbitrary dependences on (r, θ, ϕ) (in spherical coordinates). We will consider a subset of these modes which are entirely radial, without θ or ϕ dependence. One such mode, a radial breathing oscillation for which $\delta\phi^{\text{in}} = A(r^2 - R^2)$, has been set up in recent computer simulations [7]. As we discussed in Sec. III A, cold-fluid theory predicts that $\delta\phi^{\text{in}}$ can also have radial dependence $\delta\phi^{\text{in}} = f(r)$ for any function $f(r)$, and all such disturbances oscillate at frequency ω_p . The addition of correlations (or pressure terms) breaks this degeneracy and picks out a countable set of eigenfunctions for $\delta\phi(r)$.

In order to determine the frequencies and eigenfunctions we choose an appropriate complete set of radial functions, $\psi_m^{\text{in}} = r^m$, $m = 1, 2, 3, \dots$ (We will have need only of the internal form for ψ in our analysis, since $\delta\phi^{\text{out}} = 0$ for these modes.) Then the first matrix element required in Eq. (3.52) is

$$\left(\psi_n, \frac{\partial \hat{L}}{\partial \omega} \psi_m \right) \Big|_{\omega=\omega_p} = -\frac{6mn}{n+m+1} \frac{R^{n+m-2}}{\omega_p} V,$$

where $V = 4\pi R^3/3$ is the plasma volume. Here we have used Eqs. (3.26), (3.2b), and (3.2c). The matrix element involving \hat{C} is given by

specific relations between the pressure p , and the moduli κ and μ . In the strongly correlated zero-temperature limit, the following relations hold for an amorphous solid OCP at zero temperature [7]:

$$p = \frac{3\kappa}{4}, \quad \mu = -\frac{3\kappa}{10}, \quad (3.53)$$

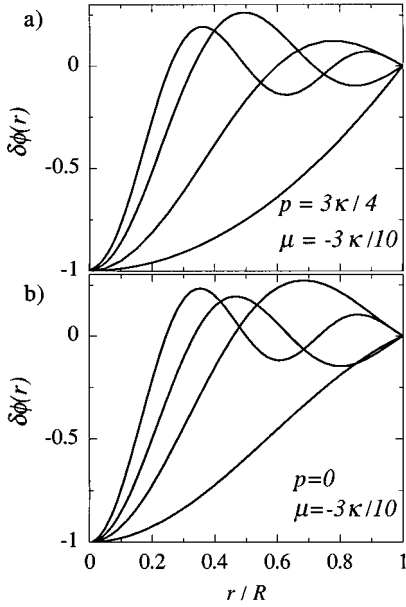


FIG. 6. First four potential eigenfunctions for spherically symmetric bulk plasma oscillations in an unmagnetized spherical plasma, for the two choices of the pressure p and moduli κ and μ shown in (a) and (b). Eigenfunctions follow from Eqs. (3.51) and (3.52). Corresponding frequencies are given by Eqs. (3.54) [(a)], and (3.56) [(b)]. Successively higher frequency shifts correspond to more oscillatory eigenfunctions. The lowest frequency eigenfunction in (a) is of the form $\delta\phi = A(r^2 - R^2)$. The eigenfunctions in (b) match the exact solution for the special case $p=0$, Eq. (B17).

so we use these relations in Eq. (3.52) as an example. One then finds that the first few numerical solutions for $\Delta\omega$ are

$$\frac{\Delta\omega}{\omega_p} \frac{Mn_0\omega_p^2 R^2}{\kappa} = 0, 9.98, 24.8, 45.5, \dots \quad (3.54)$$

and the corresponding eigenfunctions are displayed in Fig. 6(a). As the frequency shift increases, the eigenfunctions become more oscillatory. The first mode, with $\Delta\omega=0$, has a perturbed potential of the form $\delta\phi = A(r^2 - R^2)$. This result is gratifying since it matches the known exact solution for the breathing mode of a crystallized plasma sphere (see Appendix B and Sec. III A 7 of Ref. [7]). If we had chosen relations other than Eqs. (3.53), the result for $\Delta\omega$ and $\delta\phi$ would have been different [see Fig. 6(b) and below for examples], so this result provides another test of the perturbation theory.

The breathing mode has been excited in recent computer simulations of unmagnetized spherical plasmas [7]. These simulated plasmas are not necessarily held at zero temperature, so Eqs. (3.53) do not necessarily apply. While the degenerate perturbation theory can be employed to determine the frequency shift numerically as a function of T , it is also useful to obtain an approximate analytic form for the shift. Since we know that the perturbed potential at $T=0$ is $\psi = A(r^2 - R^2)$, we use this as an approximate form for the potential at finite temperature and employ it to evaluate the inner products in Eq. (3.29), since nondegenerate perturbation theory now applies. The result is

$$\Delta \frac{\omega_{\text{breathing}}}{\omega_p} = \frac{5}{2} \frac{(3\kappa - 4p)}{Mn_0\omega_p^2 R^2}. \quad (3.55)$$

This equation can also be obtained directly from Eq. (3.39). The breathing mode is the unmagnetized limit of the (2,0) upper hybrid mode in a spherical plasma. For this bulk plasma mode, $\epsilon_3 \rightarrow 0$, $\epsilon_1 \rightarrow 0$, $\sigma_1 \rightarrow 1$, $\sigma_3 \rightarrow 1$, $\epsilon_1/\epsilon_3 \rightarrow -\frac{1}{2}$, and $(\sigma_1 - \sigma_3)/\epsilon_3 = \frac{3}{2}$ [the last two relations follow by carefully evaluating the limit $\Omega_v \rightarrow 0$ in Eq. (3.11) for the (2,0) upper hybrid mode]. When these limits are substituted into Eq. (3.39), one recovers Eq. (3.55). As expected, the frequency shift vanishes at $T=0$, where Eqs. (3.53) hold. Also note that the shear modulus does not appear in Eq. (3.55) because the breathing mode is purely compressional.

We have compared Eq. (3.55) to the numerical solution of the degenerate perturbation theory at finite temperature using Eq. (2.10) for p , and using a model for the finite temperature forms of κ and μ discussed in Ref. [7]. Agreement between Eq. (3.55) and the degenerate perturbation theory is good for $\Gamma > 1$. The results are discussed in more detail in Ref. [7]. However, for arbitrary choices of p , κ , and μ the agreement between the degenerate theory and Eq. (3.55) is poor. This is because the perturbed eigenfunction remains close to $A(r^2 - R^2)$ only for physically relevant choices of p , κ , and μ . For other choices of p , κ , and μ , Eq. (3.55) does not apply, and a numerical solution of degenerate perturbation theory must be used.

In Appendix B an exact solution for the bulk plasma modes was found for the special case of a spherical unmagnetized plasma with $p=0$, but for which μ and κ are finite. In order to compare the degenerate perturbation theory for the bulk plasma modes to the exact results of Appendix B, we have also evaluated the perturbation theory frequency shifts and eigenfunctions from perturbation theory for the case $p=0$. For the numerical evaluation of Eq. (3.52) we must still choose a relation between κ and μ , so we choose the same relation as Eq. (3.53), $\mu = -3\kappa/10$. Numerical solution of Eq. (3.52) for the first four modes then yields

$$\frac{\Delta\omega}{\omega_p} \frac{Mn_0\omega_p^2 R^2}{\kappa} = 3.87, 12.9, 27.8, 48.5, \dots \quad (3.56)$$

The corresponding potential eigenfunctions are shown in Fig. 6(b). The exact dispersion relation for these radial modes, Eq. (B22), can also be solved numerically when $\mu = -3\kappa/10$, and the results for the frequency shifts are

$$\frac{\Delta\omega}{\omega_p} \frac{Mn_0\omega_p^2 R^2}{\kappa} = 3.868, 12.935, 27.794, 48.542, \dots,$$

which matches our degenerate perturbation theory. The exact potential eigenfunctions are given by Eq. (B17). The eigenfunctions also match the numerical solution of the degenerate perturbation theory [see Fig. 6(b)]. This provides another independent check on the validity of our results in the strongly correlated regime.

IV. DISCUSSION

In Sec. II we found that the moments of the density of a trapped non-neutral plasma in thermal equilibrium are

shifted slightly with respect to the values pertaining to the cold-fluid limit. The shifts arise from the change in the equilibrium density profile that occurs when correlation pressure is accounted for in the equilibrium. A general expression for the pressure shift in any density moment was derived [Eq. (2.14)]. In Sec. III we found that the shift in the equilibrium density plays a crucial role in determining the effect of correlations on the normal modes. The correlation shift of the equilibrium density shifts the mode frequencies by an amount proportional to the plasma pressure.

Elastic moduli of the strongly correlated plasma also affect the mode frequencies. Equation (3.36) provides a general expression for the frequency shift. Since the mode frequencies depend on these moduli, one could perform experiments (either real or simulated) that measure the mode frequencies in order to extract the moduli. Numerical experiments of this type will be reported in a separate paper [7]. Although the frequency shifts are small, scaling as $N^{-2/3}$, for plasmas consisting of 1000 ions this scaling implies shifts on the order of 1% which, as we will see in Ref. [7], are easily observable in the simulations, and may be observable in actual experiments.

Although several approximations based on the strongly correlated limit were made in the derivation of the mode frequency shifts, the results were found to match known exact results. For example, for the $l=1$ center of mass modes we found no frequency shift, and for the unmagnetized breathing mode we also found that the frequency shift vanished in the $T=0$ limit. In addition, the results matched an exact solution for the modes of an unmagnetized pressureless elastic sphere, discussed in Appendix B.

In addition to the plasma oscillations considered in the main body of the paper, a set of torsional oscillations was also found in the derivation of modes of an unmagnetized pressureless elastic sphere, described in Appendix B. These modes consist of twisting motions that do not change the shape or density. Thus the restoring force for these modes arises only from the shear modulus of the correlated plasma. The modes therefore have zero frequency in the cold-fluid limit, and cannot be derived using the perturbation analysis discussed in Sec. III. We leave a general discussion of the torsional modes of an unmagnetized spheroid to a separate paper. Simulation results for some of the torsional modes are presented in Ref. [7].

It is tempting to apply our results for the frequency shifts to the weakly correlated regime. However, while Eqs. (3.36)–(3.50) provide predictions for the shifts in this regime, i.e., $\Delta\omega = Tf(\alpha)/N^{2/3}$ for some function f which differs for different modes, our derivation is no longer valid. This is because for weak correlation the equilibrium density profile now extends beyond the cold-fluid profile (see Fig. 1), so none of the approximations discussed in the derivation of Eq. (3.35) apply. Our derivation can be justified only in the strongly correlated limit where the equilibrium density has shrunk inside the cold-fluid profile.

However, it appears both from experiments [3] and simulations [3, 27] that finite pressure corrections to the mode frequencies in the weakly correlated limit do have the approximate form of the equations derived here [at least for the (2,0) mode]. Of course, in the weakly correlated limit the warm-fluid equations describing the non-neutral plasma

equilibrium and dynamics are well posed, and can be solved without approximations, at least in principle. However, extraction of the frequency shift from the warm-fluid equations in the weakly correlated regime turns out to be a surprisingly difficult theoretical problem. It appears that perturbation techniques of the type employed in this paper do not apply, and a more powerful boundary layer calculation may be required. Nevertheless, the results of our perturbation theory, such as the form of the perturbed eigenfunctions (see Figs. 5 and 6, for example) may provide useful intuition in any future analysis.

ACKNOWLEDGMENTS

The author gratefully acknowledges stimulating discussions with Professor R. L. Spencer. This work was supported by National Science Foundation Grant Nos. PHY91-20240 and PHY94-21318, and an Office of Naval Research Grant No. N00014-89-J-1714.

APPENDIX A: MOMENTS OF EQUILIBRIUM DENSITY FROM THE BBGKY HIERARCHY

In this appendix we evaluate the integral appearing in Eq. (2.13). We do so by considering the first equation of the equilibrium BBGKY hierarchy for the case of a spherical plasma (i.e., $\beta=1$). The derivation is similar to that of Tot-suji for the contact density of an electrolyte at the wall of a container [28]. For a harmonically trapped non-neutral plasma, the first equation of the equilibrium BBGKY hierarchy can be derived by differentiating the Gibb's distribution f of Eq. (2.1) with respect to r_1 , multiplying by N , and then integrating over all other variables. The result is

$$kT \frac{\partial n}{\partial r_1}(r_1; \Gamma) = -qn(r_1; \Gamma) \frac{\partial}{\partial r_1} [\phi_p(r_1) + \phi_e(r_1)] - q^2 \int d^3x_2 g(\mathbf{x}_1, \mathbf{x}_2; \Gamma) \frac{\partial}{\partial r_1} |\mathbf{x}_1 - \mathbf{x}_2|^{-1}, \quad (\text{A1})$$

where ϕ_e is defined in Eq. (2.1b), ϕ_p is the plasma potential defined by $\nabla^2 \phi_p = -4\pi qn(r; \Gamma)$, and where $g(\mathbf{x}_1, \mathbf{x}_2; \Gamma)$ is the two-particle correlation function, related to the Gibb's distribution through

$$g(\mathbf{x}_1, \mathbf{x}_2; \Gamma) = N^2 \int d^3x_3 \dots d^3x_N d^3v_1 \dots d^3v_N \times f(\mathbf{x}_1, \dots, \mathbf{x}_N, \mathbf{v}_1, \dots, \mathbf{v}_N) - n(\mathbf{x}_1; \Gamma)n(\mathbf{x}_2; \Gamma).$$

We integrate Eq. (A1) in radius from a point $r_1 = r_{\text{in}}$ within the plasma where the single-particle density is uniform, $n(r_{\text{in}}; \Gamma) = n_0$, to a point $r_1 = r_{\text{out}}$, where the density has fallen to zero:

$$\begin{aligned}
-kTn_0 &= -q \int_{r_{\text{in}}}^{r_{\text{out}}} dr_1 n(r_1; \Gamma) \frac{\partial}{\partial r_1} (\phi_p + \phi_e) \\
&\quad - q^2 \int_{r_{\text{in}}}^{r_{\text{out}}} dr_1 \int d^3x_2 g(\mathbf{x}_1, \mathbf{x}_2; \Gamma) \frac{\partial}{\partial r_1} |\mathbf{x}_1 - \mathbf{x}_2|^{-1}.
\end{aligned} \tag{A2}$$

We first consider the second term involving the correlation function. Assuming that the radius of the plasma is large compared to the correlation length, we approximate the plasma surface by a planar interface, in which case $g(\mathbf{x}_1, \mathbf{x}_2; \Gamma) = g(r_1, r_2, |\mathbf{x}_{\perp 1} - \mathbf{x}_{\perp 2}|; \Gamma)$, where \mathbf{x}_{\perp} is a 2D position parallel to the plane of the interface. This approximation neglects the effects of surface tension due to curvature of the surface, and assumes that g is isotropic in the parallel plane, as in the fluid or glass phases. We then split the integral over r_2 in Eq. (A2) into two pieces:

$$\begin{aligned}
& q^2 \int_{r_{\text{in}}}^{r_{\text{out}}} dr_1 \int d^3x_2 g \frac{\partial}{\partial r_1} |\mathbf{x}_1 - \mathbf{x}_2|^{-1} \\
&= q^2 \int_{r_{\text{in}}}^{r_{\text{out}}} dr_1 \int_0^{r_{\text{in}}} dr_2 \int d^2\mathbf{x}_{\perp 2} g(r_1, r_2, |\mathbf{x}_{\perp 1} - \mathbf{x}_{\perp 2}|) \\
&\quad \times \frac{\partial}{\partial r_1} |\mathbf{x}_1 - \mathbf{x}_2|^{-1} + q^2 \int_{r_{\text{in}}}^{r_{\text{out}}} dr_1 \int_{r_{\text{in}}}^{r_{\text{out}}} dr_2 \\
&\quad \times \int d^2\mathbf{x}_{\perp 2} g(r_1, r_2, |\mathbf{x}_{\perp 1} - \mathbf{x}_{\perp 2}|) \frac{\partial}{\partial r_1} |\mathbf{x}_1 - \mathbf{x}_2|^{-1}.
\end{aligned}$$

However, the second integral vanishes, since g is symmetric under interchange of r_1 and r_2 , but the force $-q^2 \partial/\partial r_1 |\mathbf{x}_1 - \mathbf{x}_2|^{-1}$ is antisymmetric. Furthermore, in the first integral r_{in} is chosen in the bulk, so we may replace g by $g(|\mathbf{x}_1 - \mathbf{x}_2|; \Gamma)$, the correlation function for a homogeneous one-component plasma. It is then not difficult to show that the first integral equals $-n_0 U/3N$, where U is the correlation energy of a one-component plasma, defined by [28]

$$\frac{U}{NkT}(\Gamma) = \frac{3\Gamma}{2} \int_0^{\infty} \frac{r dr}{a_{\text{WS}}^2} \frac{g(r; \Gamma)}{n_0^2}.$$

Using this result in Eq. (A2) yields

$$p = q \int_{r_{\text{in}}}^{r_{\text{out}}} dr_1 n(r_1; \Gamma) \frac{\partial}{\partial r_1} (\phi_p + \phi_e), \tag{A3}$$

where $p \equiv n_0 kT(1 + U/3NkT)$ is the bulk thermal pressure of the OCP, including the ideal gas contribution [see Eq. (2.10)]. Thus the bulk pressure is related to a difference that develops between the plasma potential ϕ_p and the effective confining potential ϕ_e near the plasma edge. Recall that $\phi_p + \phi_e = \text{const}$ within a cold-fluid plasma when pressure is neglected.

Now, since the plasma is assumed to be spherically symmetric, $\partial\phi_p/\partial r$ is given by

$$\frac{\partial\phi_p}{\partial r} = -\frac{4\pi q}{r^2} \left[\int_{r_{\text{in}}}^r r^2 dr n + \frac{n_0 r_{\text{in}}^3}{3} \right].$$

We substitute this relation into Eq. (A3), then change integration variables from r to $u \equiv r - r_{\text{in}}$. The variable u is the distance from the fluid plasma edge. We then expand in powers of u/r_{in} , yielding, after some algebra,

$$\begin{aligned}
p &= 2\pi q^2 \left[2n_0 \int_0^{\infty} du u \bar{n}(u; \Gamma) - \left(\int_0^{\infty} du \bar{n}(u; \Gamma) \right)^2 \right] \\
&\quad + O(1/r_{\text{in}}),
\end{aligned} \tag{A4}$$

where $\bar{n}(u; \Gamma) \equiv n(r_{\text{in}} + u; \Gamma)$ is the density at the plasma edge.

If we define a difference $\Delta n(u; \Gamma) = \bar{n}(u; \Gamma) - n_f(r_{\text{in}} + u)$ between the equilibrium density and the cold-fluid profile, Eq. (A4) simplifies to

$$p = 4\pi q^2 n_0 \int_{-\infty}^{\infty} du u \Delta n(u; \Gamma), \tag{A5}$$

where we can now extend the lower limit to $-\infty$ since $\Delta n(u; \Gamma)$ is zero at large $|u|$. In the derivation of (A5) we have used the relation $\int_{-\infty}^{\infty} du \Delta n = 0$.

APPENDIX B: TESTS OF THE PERTURBATION THEORY

In this appendix we test the validity of our perturbation theory results in two ways. First, we evaluate a general expression for the perturbed potential eigenfunction $\Delta\psi$ of Eq. (3.28), and show that it is indeed small compared to ψ in a strongly correlated plasma. Second, we compare our results to an exact solution of Eqs. (3.15), (3.20), and (3.21), adapted from the original derivation of Love, for the case of a uniform unmagnetized elastic sphere [29].

1. Perturbed eigenfunction

In order to calculate the perturbed eigenfunction $\Delta\psi$ in the most straightforward manner, we return for a moment to the momentum equation, Eq. (3.22). Equation (3.16) implies that a term of the form $\nabla(\delta\mathbf{x} \cdot \nabla p)$ appears on the right-hand side of Eq. (3.22), arising from $\nabla \cdot \delta\pi$. Within the plasma, where $n^{(0)}$ is constant, we can combine $-qn^{(0)}\nabla\delta\phi$ with this term, yielding $-qn^{(0)}\nabla(\delta\phi - \delta\mathbf{x} \cdot \nabla p/qn_0)$. We therefore expect a first-order pressure correction in $\Delta\psi$ of the form $\delta\mathbf{x}_f \cdot \nabla p/qn_0$, where $\delta\mathbf{x}_f$ is the fluid displacement defined in Eq. (3.34). It will be easiest to subtract out this correction initially. Therefore we define

$$\Delta\bar{\psi} = \Delta\psi - \delta\mathbf{x}_f \cdot \nabla p/qn_0,$$

and we replace $\Delta\psi$ with $\Delta\bar{\psi}$ in Eq. (3.28), yielding

$$\hat{L}\Delta\bar{\psi} + \Delta\omega \frac{\partial\hat{L}}{\partial\omega} \psi = \hat{C}\psi - \hat{L} \frac{\delta\mathbf{x}_f \cdot \nabla p}{qn_0}. \tag{B1}$$

We then expand $\Delta\bar{\psi}$ in the orthonormal eigenfunctions χ_n of \hat{L} :

$$\Delta\bar{\psi} = \sum_n' a_n \chi_n, \quad (\text{B2})$$

where the χ_n 's satisfy

$$\hat{L}\chi_n = \lambda_n \chi_n \quad (\text{B3})$$

for a set of eigenvalues λ_n . One eigenvalue is $\lambda_n = 0$, corresponding to $\chi_n = \psi$, and the prime on the sum in Eq. (B2) means the sum does not include this eigenfunction. The coefficients a_n are obtained by taking the inner product of Eq. (B1) with χ_n :

$$a_n = [(\chi_n, \hat{C}\psi) - (\chi_n, \hat{L}\delta\mathbf{x}_f \cdot \nabla p) / qn_0 - \Delta\omega(\chi_n, \partial\hat{L}/\partial\omega\psi)] / \lambda_n^*. \quad (\text{B4})$$

Writing the first two inner products in Eq. (B4) as integrals, and using Eqs. (3.26) and (3.27), yields

$$\begin{aligned} & (\chi_n, \hat{C}\psi) - (\chi_n, \hat{L}\delta\mathbf{x}_f \cdot \nabla p) / qn_0 \\ &= - \int d^3x \left\{ \Delta\bar{n} \nabla \chi_n^* \cdot \sigma \cdot \nabla \psi + \nabla^2 \psi \frac{\delta\mathbf{x}_n^* \cdot \nabla p}{qn^{(0)}} \right. \\ & \quad \left. + \lambda_n^* \chi_n^* \frac{\delta\mathbf{x}_f \cdot \nabla p}{qn_0} + 4\pi \delta\mathbf{x}_n^* \cdot \nabla \cdot \delta\pi \right\}, \end{aligned}$$

where $\delta\mathbf{x}_n = \sigma \cdot \nabla \chi_n / 4\pi qn_0$ is the fluid displacement due to the eigenfunction χ_n , and where we have used the Hermitian property of \hat{L} together with Eq. (B3).

Then, after integrating by parts on the last term, we obtain

$$\begin{aligned} & - \int d^3x \left\{ \Delta\bar{n} \cdot \nabla \chi_n^* \cdot \sigma \cdot \nabla \psi^{\text{in}} + \frac{\delta\mathbf{x}_n^* \cdot \nabla p \nabla^2 \psi^{\text{in}}}{qn_0} \right. \\ & \quad + \lambda_n^* \chi_n^* \frac{\delta\mathbf{x}_f \cdot \nabla p}{qn_0} + \frac{\delta\mathbf{x}_f \cdot \nabla p}{qn_0} \nabla \cdot (\sigma \cdot \nabla \chi_n)^* \\ & \quad \left. + 4\pi u_{ijn}^* s_{ij} \right\}, \quad (\text{B5}) \end{aligned}$$

where u_{ijn} equals u_{ij} given by Eq. (3.18) with $\delta\mathbf{x} = \delta\mathbf{x}_n$, and where we have employed the same approximations as in the derivation of Eq. (3.35), dropping surface terms in the integrals and keeping terms only to linear order in gradients of the pressure and density.

Let us consider the size of various terms in Eq. (B5). The stress tensor s_{ij} varies in space within the plasma on a relatively slow spatial scale given by $\psi(\mathbf{x})$, so $\int d^3x u_{ijn}^* s_{ij}$ will approach zero like $\lambda_n^{-1/2}$ for large n because χ_n becomes rapidly varying. Thus this contribution to the sum in Eq. (B2) is convergent for large n . (We will see examples of this behavior in Appendix B 2.) However, since ∇p varies rapidly near the plasma edge, it is not obvious that the other terms in Eq. (B5), involving bulk pressure gradients, provide a convergent sum for $\Delta\bar{\psi}$, so we will consider these terms more carefully.

The first term in Eq. (B5) can be related to the thermal pressure using Eq. (2.14):

$$\int d^3x \Delta\bar{n} \nabla \chi_n^* \cdot \sigma \cdot \nabla \chi_n = \frac{pN}{M\omega_p^2 n_0^2} \langle \nabla^2 (\nabla \chi_n^* \cdot \sigma \cdot \nabla \chi_n) \rangle_f.$$

Application of Gauss's law then yields

$$\begin{aligned} & \int d^3x \Delta\bar{n} \nabla \chi_n^* \cdot \sigma \cdot \nabla \psi \\ &= \frac{p}{4\pi q^2 n_0^2} \int d^2x \hat{\mathbf{u}} \cdot \nabla (\nabla \chi_n^* \cdot \sigma \cdot \nabla \psi), \end{aligned}$$

where the integral over d^2x runs over the surface of the fluid spheroid, and $\hat{\mathbf{u}}$ is a unit vector normal to the surface. The second, third, and fourth terms of Eq. (B5) can also be related to surface integrals since in thermal equilibrium p is uniform within the plasma and zero outside of it, so ∇p is sharply peaked at the surface. Furthermore, in the fourth term we use Eq. (B3) to write $\nabla \cdot (\sigma \cdot \nabla \chi_n)^* = -\lambda_n^* \chi_n^* + \nabla^2 \chi_n^*$, so after a cancellation the first four terms of Eq. (B5) become

$$\begin{aligned} & - \int d^2x \frac{p}{qn_0} \left\{ \hat{\mathbf{u}} \cdot \nabla \left(\nabla \chi_n^* \cdot \frac{\sigma}{4\pi qn_0} \cdot \nabla \psi^{\text{in}} \right) \right. \\ & \quad \left. - \frac{\hat{\mathbf{u}} \cdot \sigma^* \cdot \nabla \chi_n^* \nabla^2 \psi^{\text{in}}}{4\pi qn_0} - \hat{\mathbf{u}} \cdot \delta\mathbf{x}_f \nabla^2 \chi_n^* \right\}. \end{aligned}$$

The second term, involving $\sigma^* \cdot \nabla \chi_n^*$, has only a single gradient of χ_n , so this term is of order $\sqrt{\lambda_n} \chi_n$ in the large n limit. Thus, when divided by λ_n^* in order to obtain a_n in Eq. (B4), it provides a convergent term in the large n limit. However, the first and third terms involve two derivatives of χ_n , which can produce a term of order $\lambda_n \chi_n$ in the large n limit. Since ψ^{in} varies slowly along the surface of the plasma, the surface integral picks out only those χ_n with an equally slow variation along the surface. Thus the largest term in $\nabla^2 \chi_n^*$ is $d^2 \chi_n^* / ds^2$. Similarly, the largest term in $\hat{\mathbf{u}} \cdot \nabla (\nabla \chi_n^* \cdot (\sigma / 4\pi qn_0) \cdot \nabla \psi^{\text{in}})$ is $(d^2 \chi_n^* / ds^2) (\hat{\mathbf{u}} \cdot \delta\mathbf{x}_f)$, and this term cancels the third term, leaving only convergent contributions to Eq. (B4).

The hat only remaining contribution to a_n , $\Delta\omega(\chi_n, \partial\hat{L}/\partial\omega\psi) / \lambda_n^*$, is also easily shown to yield a convergent sum in the large n limit through a similar argument to that used for the other terms. Using Eq. (3.26) for \hat{L} , integration by parts yields

$$(\chi_n, \partial\hat{L}/\partial\omega\psi) = \int_{\text{in}} d^3x \nabla \chi_n^* \cdot \partial\sigma/\partial\omega \nabla \psi^{\text{in}},$$

and, since $\partial\sigma/\partial\omega$ is slowly varying within the plasma, the integral phase mixes away for large n due to the relatively slow variation of ψ^{in} compared to χ_n .

We have shown that Eq. (B2) for $\Delta\bar{\psi}$ is a convergent sum with coefficients proportional to the pressure corrections. Our perturbation theory therefore should provide sensible results for the frequency shifts, provided that the approximations leading to Eq. (B5) are valid. We will next consider the functional form for $\Delta\bar{\psi}$ for a specific case.

Unmagnetized (2,0) mode in a spherical plasma

Let us consider the perturbed eigenfunctions for the case of an unmagnetized spherical plasma. It is evident from Eqs. (B2), (B4), (B5), (3.19a), and (3.37) that $\Delta\bar{\psi}$ breaks into a part proportional to pressure p and one proportional to bulk and shear moduli. We first consider the part proportional to bulk and shear moduli, dropping the pressure terms. In this case Eq. (B4) becomes

$$a_n = \int_{\text{in}} d^3x \left\{ 4\pi u_{ij}^* s_{ij} - 2 \frac{\Delta\omega\omega^2}{\omega^3} \nabla\chi_n^* \cdot \nabla\psi^{\text{in}} \right\} / \lambda_n^*, \quad (\text{B6})$$

where s_{ij} is determined by ψ^{in} via Eqs. (3.18), (3.19a), and (3.34), where we have used the unmagnetized limit for $\partial\sigma/\partial\omega$ [see Eq. (3.23)], and where the part of $\Delta\omega$ independent of pressure p can be obtained from Eq. (3.37).

Now, for a spherical plasma the eigenfunctions χ_n obey a scalar Helmholtz equation with a separable solution in spherical coordinates:

$$\varepsilon_3 \nabla^2 \chi_n^{\text{in}} = \lambda_n \chi_n^{\text{in}}, \quad (\text{B7a})$$

$$\nabla^2 \chi_n^{\text{out}} = \lambda_n \chi_n^{\text{out}}, \quad (\text{B7b})$$

with continuity conditions at the plasma edge $r=R$ given by

$$\chi_n^{\text{in}} = \chi_n^{\text{out}}$$

and

$$\varepsilon_3 \partial\chi_n^{\text{in}}/\partial r = \partial\chi_n^{\text{out}}/\partial r.$$

Note that Eq. (3.8) implies that ε_3 is a fixed negative number for the surface plasma modes, $\varepsilon_3 = -(l+1)/l$ for given mode numbers (l, m) . Thus we must find the set of χ_n 's and λ_n 's which solve Eqs. (B7) subject to boundary conditions that $\chi_n=0$ at $r=R_w$, where R_w is the radius of a spherical conducting wall placed outside the plasma.

We choose R_w to be a large but finite distance from the plasma since there are two types of eigenfunctions: plasma modes whose potential falls off rapidly outside the plasma, and vacuum modes which exist mainly between the wall and the plasma. The set of eigenvalues λ_n for the vacuum modes becomes a continuum in the limit that $R_w \rightarrow \infty$, so it is easier to take R_w large but finite.

The plasma mode solutions fall off rapidly outside the plasma, so we may neglect image charge effects. The plasma solutions of Eq. (B7) are then

$$\chi_n^{(\text{in})} = A j_u(\sqrt{\lambda_{uk}/|\varepsilon_3|}r) P_u^s(\cos\theta) e^{is\phi},$$

$$\chi_n^{(\text{out})} = B k_u(\sqrt{-\lambda_{uk}}r) P_u^s(\cos\theta) e^{is\phi},$$

where $j_u(x)$ is a spherical Bessel function of the first kind, $k_u(x)$ is a modified spherical Bessel function of the third kind, and P_u^s is the usual Legendre function. The index u must obey $u \geq |s|$. For given u there is a countable set of solutions for λ , and the index k determines which solution for λ_{uk} is used. Thus, the index n on χ_n really consists of the three integers (u, k, s) . The eigenvalue equation for λ_{uk} follows from Eqs. (B7b),

$$-\sqrt{|\varepsilon_3|} \frac{j'_u}{j_u} = \frac{k'_u}{k_u} \Big|_{r=R}, \quad (\text{B8})$$

where the prime denotes differentiation with respect to the entire argument. It is not difficult to show that a solution exists for $\lambda_{uk}=0$, corresponding to the fluid eigenfunction ψ . We are to neglect this solution since we keep only χ_n 's which are orthogonal to ψ in the sum in Eq. (B2).

The vacuum solutions to Eqs. (B7) are of a similar form,

$$\chi_n^{\text{in}} = A i_u(\sqrt{-\lambda_{uk}/|\varepsilon_3|}r) P_u^s(\cos\theta) e^{is\phi},$$

$$\chi_n^{\text{out}} = B \left[y_u(\sqrt{-\lambda_{uk}}r) - \frac{y_u(\sqrt{-\lambda_{uk}}R_w)}{j_u(\sqrt{-\lambda_{uk}}R_w)} j_u(\sqrt{-\lambda_{uk}}r) \right] P_u^s(\cos\theta) e^{is\phi},$$

where $i_u(x)$ is a modified spherical Bessel function of the second kind, and where $y_u(x)$ is a spherical Bessel function of the second kind. An eigenvalue equation similar to Eq. (B8) can be obtained for $\sqrt{-\lambda_{uk}}$. Just as for the plasma modes a solution exists for $\lambda_{uk}=0$, equal to the fluid eigenfunction ψ ; we neglect this solution as we keep only those eigenfunctions orthogonal to ψ in Eq. (B2).

Using these eigenfunctions we have evaluated the a_n 's for the case of the (2,0) mode. Using Eq. (B6), it is not difficult to show that the only eigenfunctions which yield nonvanishing a_n 's are those for which $u=2$ and $s=0$, so the dependence of $\Delta\bar{\psi}$ on θ and ϕ is the same as that of the fluid mode. Furthermore $\nabla^2\psi^{\text{in}}=0$, so only shear stress contributions proportional to μ appear in s_{ij} [see Eqs. (3.19a) and (3.34)], and therefore Eq. (B6) implies that $\Delta\bar{\psi}$ is proportional to μ and independent of κ . Then after numerically solving for the eigenvalues λ_{2k} we have summed the series in Eq. (B2) to obtain the radial dependence of $\Delta\bar{\psi}$, keeping a large but finite number of eigenfunctions (62 plasma eigenfunctions and 57 vacuum eigenfunctions). Thus the part of $\Delta\bar{\psi}$ proportional to μ has the form

$$\Delta\bar{\psi} = \frac{\mu}{M n_0 \omega_p^2 R^2} \psi(R, \theta) f(r), \quad (\text{B9})$$

where $\psi(r, \theta)$ is the (2,0) fluid mode potential and $f(r)$ is the dimensionless function that results from summing the plasma and vacuum eigenfunctions. The result for $f(r)$ is shown in Fig. 5. In the upper figure the plasma and vacuum eigenfunction contributions to $f(r)$ are shown separately; they are added together to provide the full $f(r)$ shown in the lower figure. Note that a discontinuity in $f(r)$ appears at the plasma edge. The physical reason for the discontinuity is discussed in Appendix B 2. The small oscillations in the potential are a consequence of truncation of the sum in Eq. (B2); by keeping more terms the oscillations can be suppressed further.

Next, we return to Eq. (B4) and evaluate the part of $\Delta\bar{\psi}$ proportional to thermal pressure p . This involves an evaluation of the surface integrals in Eq. (B5). The integrals pick out only those eigenfunctions χ_n for which $u=2$ and $s=0$, just as before. After adding in the contribution to a_n from the

pressure term in $\Delta\psi$ [see Eq. (3.41)], we find that the part of $\Delta\psi$ proportional to pressure p has the same functional form as the part proportional to μ that is displayed in Fig. 5. The only difference between these two parts is a numerical factor. The part of $\Delta\psi$ proportional to p has the form

$$\Delta\bar{\psi} = \frac{2}{5} \frac{p}{Mn_0\omega_p^2 R^2} \psi(R, \theta) f(r), \quad (\text{B10})$$

where $f(r)$ is the same dimensionless function as in Eq. (B9), displayed in Fig. 5.

2. An exact solution

As a final test of the perturbation theory, we will now compare the approximate perturbation results to an exact solution for a special case. We return to Eq. (3.15) and take $\Omega_v = p = 0$ but retain the bulk and shear moduli. We will further assume the equilibrium is a uniform density sphere, which is consistent with the assumption $p = 0$. Then within the sphere Eq. (3.15) becomes

$$-\omega^2 Mn_0 \delta\mathbf{x} = -qn_0 \nabla \delta\phi + \mu \nabla^2 \delta\mathbf{x} + (\kappa + \frac{1}{3}\mu) \nabla(\nabla \cdot \delta\mathbf{x}). \quad (\text{B11})$$

Furthermore, the boundary condition $\hat{\mathbf{r}} \cdot \delta\pi = 0$ must be met at the surface of the sphere. In spherical coordinates this condition becomes the three equations

$$(\kappa - \frac{2}{3}\mu) \nabla \cdot \delta\mathbf{x} + 2\mu \frac{\partial \delta x_r}{\partial r} = 0, \quad (\text{B12a})$$

$$\frac{\partial \delta x_r}{\partial \theta} + R \frac{\partial \delta x_\theta}{\partial r} - \delta x_\theta = 0, \quad (\text{B12b})$$

$$\frac{1}{\sin\theta} \frac{\partial \delta x_r}{\partial \phi} + R \frac{\partial \delta x_\phi}{\partial r} - \delta x_\phi = 0 \quad (\text{B12c})$$

for the components of $\delta\mathbf{x}$ in the r , θ , and ϕ directions at $r = R$. In addition to these equations we have the boundary condition that $\delta\phi \rightarrow 0$ at $r \rightarrow \infty$.

Equations (B11) and (B12), together with the continuity and Poisson equations, Eqs. (3.20) and (3.21), can be solved exactly, as was first shown by Love in 1911 [29]. Writing $\delta\mathbf{x}$ as a sum of a curl free and divergence free field,

$$\delta\mathbf{x} = \nabla g + \nabla \times \mathbf{h}, \quad (\text{B13})$$

we first take the divergence of Eq. (B11),

$$-\omega^2 Mn_0 \nabla^2 g = (\kappa + \frac{4}{3}\mu) \nabla^2 \nabla^2 g - 4\pi q^2 n_0^2 \nabla^2 g.$$

This is a scalar Helmholtz equation for $\nabla^2 g$, so g may be decomposed into a solution to this wave equation and a solution to $\nabla^2 g = 0$:

$$g = [A j_l(k_1 r) + B r^l] P_l^m(\cos\theta) e^{im\phi}, \quad (\text{B14})$$

where $k_1 = \sqrt{(\omega^2 - \omega_p^2) Mn_0 / (\kappa + 4/3\mu)}$, and $j_l(x)$ is a spherical Bessel function.

Returning to Eq. (B11), we now take the curl of the equation, noting that \mathbf{h} is determined only up to the gradient of a

scalar so we are free to choose $\nabla \cdot \mathbf{h} = 0$. The result is a vector Helmholtz equation in $\nabla^2 \mathbf{h}$:

$$\omega^2 Mn_0 \nabla^2 \mathbf{h} = -\mu \nabla^2 \nabla^2 \mathbf{h}.$$

The solution for \mathbf{h} is a sum of a solution to this wave equation and to the vector Laplace equation $\nabla^2 \mathbf{h} = 0$. We keep only the solutions which obey $\nabla \cdot \mathbf{h} = 0$,

$$\mathbf{h} = -C \mathbf{r} \times \nabla [j_l(k_2 r) P_l^m e^{im\phi}] + D \nabla [\mathbf{r} \nabla (j_l(k_2 r) P_l^m e^{im\phi})] + E \mathbf{r} \times \nabla (r^l P_l^m e^{im\phi}), \quad (\text{B15})$$

where $P_l^m = P_l^m(\cos\theta)$ and $k_2 = \sqrt{\omega^2 Mn_0 / \mu}$. Furthermore, the continuity equation, Eq. (3.20), and the Poisson equation, Eq. (3.21), can be combined with Eq. (B13) to yield

$$\nabla^2 \delta\phi^{\text{in}} = 4\pi q n_0 \nabla^2 g,$$

which has the solution

$$\delta\phi^{\text{in}} = 4\pi q n_0 (g + F r^l P_l^m e^{im\phi}). \quad (\text{B16})$$

Equations (B13)–(B16) must also obey the original equation for $\delta\mathbf{x}$, Eq. (B11). This implies relations between the coefficients $A \dots F$, as we will see. Substitution of Eqs. (B13)–(B16) into Eq. (B11) yields

$$\begin{aligned} & [(\omega_p^2 - \omega^2)B + \omega_p^2 F] \nabla (r^l P_l^m e^{im\phi}) \\ & + E \left[2 \nabla (r^l P_l^m e^{im\phi}) + r \frac{\partial}{\partial r} \nabla (r^l P_l^m e^{im\phi}) \right] = 0. \end{aligned}$$

This equation can only be satisfied for $E = 0$ and $F = (\omega^2 - \omega_p^2)B / \omega_p^2$. When these results, together with Eq. (B14), are used in Eq. (B16), we find the following form for the interior potential:

$$\delta\phi^{\text{in}} = 4\pi q n_0 \left(A j_l(k_1 r) + \frac{\omega^2}{\omega_p^2} B r^l \right) P_l^m e^{im\phi}. \quad (\text{B17})$$

This solution for the perturbed potential must be matched across the plasma vacuum boundary to a solution to $\nabla^2 \delta\phi^{\text{out}} = 0$. The matching conditions are

$$\delta\phi^{\text{in}} = \delta\phi^{\text{out}}|_{r=R} \quad (\text{B18a})$$

and

$$\frac{\partial \delta\phi^{\text{out}}}{\partial r} - \frac{\partial \delta\phi^{\text{in}}}{\partial r} = -4\pi q n_0 \delta x_r|_{r=R}, \quad (\text{B18b})$$

which follows because movement of the plasma surface by δx_r is equivalent to a surface charge. The outer solution for $\delta\phi$ is

$$\delta\phi^{\text{out}} = 4\pi q n_0 G r^{-(l+1)} P_l^m e^{im\phi}. \quad (\text{B19})$$

Torsional modes

We therefore need to solve for five independent constants A , B , C , D , and G , via the five equations (B12) and (B18).

We can reduce the number of equations and unknowns further by evaluating $\delta\mathbf{x}$ in spherical coordinates using Eqs. (B13)–(B15):

$$\begin{aligned}\delta x_r &= \{A j_1' + l B r^{l-1} + C[l(l+1)j_2]\} P_l^m e^{im\phi}, \\ \delta x_\theta &= \left\{ A \frac{j_1}{r} + B r^{l-1} + C[j_2' + j_2/r] \right\} e^{im\phi} \frac{\partial}{\partial \theta} P_l^m \\ &\quad - D \frac{k_2^2 j_2}{\sin \theta} P_l^m i m e^{im\phi}, \\ \delta x_\phi &= \left\{ A \frac{j_2}{r} + B r^{l-1} + C[j_2' + j_2/r] \right\} \frac{P_l^m}{\sin \theta} i m e^{im\phi} \\ &\quad + D k_2^2 j_2 e^{im\phi} \frac{\partial P_l^m}{\partial \theta},\end{aligned}\quad (\text{B20})$$

where we have introduced the shorthand $j_1 \equiv j_1(k_1 r)$, $j_2 \equiv j_l(k_2 r)$, and primes refer to differentiation with respect to r . Two sets of solutions now separate out. For one set $D=0$, and for the other set $A=B=C=G=0$. The latter are referred to as torsional, or toroidal modes. They have not appeared in our previous discussions because they cannot be obtained from perturbation theory. This is because their cold-fluid analogs have zero frequency. These modes are torsional oscillations of the sphere which do not give rise to shape changes or density perturbations. The only restoring force for these modes comes from the shear modulus, and it is for this reason that the modes do not exist in the fluid limit.

For the torsional modes Eqs. (B20) imply $\delta x_r = 0$ and $\nabla \cdot \delta \mathbf{x} = 0$. Furthermore, Eqs. (B17) and (B18) imply $\delta \phi = 0$. Then the two boundary conditions Eqs. (B12b) and (B12c) are identical and provide the dispersion relation

$$R \frac{\partial}{\partial R} j_l(k_2 R) = j_l(k_2 R).$$

We will see in a following paper [7] that these modes can be observed in simulations of unmagnetized strongly correlated non-neutral plasmas.

Bulk plasma modes

Now we turn to the other sets of modes for which $D=0$. For these modes the position change $\delta\mathbf{x}$ causes a perturbed potential $\delta\phi$. There are four unknowns (A, B, C, G) and four equations, Eqs. (B18), (B12a), and (B12b), since the boundary conditions Eqs. (B12b) and (B12c) are identical in this case. The resulting dispersion relation is quite complex: we leave it in the form of three coupled homogeneous equations for A , B , and C :

$$A(l+1) \frac{j_1}{R} + B R^{l-1} \left[(2l+1) \frac{\omega^2}{\omega_p^2} - l \right] - C \frac{l(l+1)}{R} j_2 = 0, \quad (\text{B21a})$$

$$\begin{aligned}A \left[j_1'' + \frac{1}{2} \left(\frac{2}{3} - \frac{\kappa}{\mu} \right) k_1^2 j_1 \right] + B l(l-1) R^{l-2} \\ + C \frac{l(l+1)}{R} \left(j_2' - \frac{j_2}{R} \right) = 0,\end{aligned}\quad (\text{B21b})$$

$$\begin{aligned}A \left[j_1' - \frac{j_1}{R} \right] + B l(l-1) R^{l-2} \\ + C \left[-j_2' + \left(\frac{l(l+1)-1}{R} - \frac{k_2^2 R}{2} \right) j_2 \right] = 0,\end{aligned}\quad (\text{B21c})$$

where primes denote derivatives with respect to R , and here $j_1 \equiv j_l(k_1 R)$ and $j_2 \equiv j_l(k_2 R)$. Solution of these three coupled equations must be carried out numerically, except for a few special cases. For $l=0$, Eq. (B21b) implies that

$$j_0'' + \frac{1}{2} \left(\frac{2}{3} - \frac{\kappa}{\mu} \right) k_1^2 j_0(k_1 R) = 0,$$

which is the dispersion relation for a set of spherically symmetric modes. These modes correspond to the bulk plasma oscillations discussed in Sec. III. In fluid theory, these bulk modes are degenerate with frequencies equal to the plasma frequency. Addition of bulk and shear moduli breaks the degeneracy. The dispersion relation can also be written in terms of elementary functions:

$$1 - k_1^2 R^2 \frac{\kappa + \frac{4}{3}\mu}{4\mu} = k_1 R \cot k_1 R, \quad (\text{B22})$$

which has a countably infinite set of solutions for $k_1 R$. Now, one can show that for a strongly correlated plasma $(\kappa + 4/3\mu)/M n \omega_p^2 \sim O(a_{\text{WS}}^2)$. Thus, as $R/a_{\text{WS}} \rightarrow \infty$ (the fluid limit), Eq. (B22) implies that all the mode frequencies approach ω_p like a_{WS}^2/R^2 , as expected from the results of fluid theory for the bulk plasma modes in the unmagnetized limit.

Surface plasma modes

The other case for which Eqs. (B21) simplify is the fluid limit, $R/a_{\text{WS}} \rightarrow \infty$. In this case $k_2 R \rightarrow \infty$, and $k_1 R$ also approaches infinity provided that ω is unequal to ω_p in the limit. As $k_1 R$ and $k_2 R$ become large, Eqs. (B21b) and (B21c) imply that A and C approach zero, leaving only B finite, and then Eq. (B21a) implies $\omega^2 = \omega_p^2 l/(2l+1)$, the cold-fluid limit for the surface modes [Eq. (3.81)].

In order to compare our perturbation results for the mode frequencies to the exact solution for the frequencies of the surface modes, we have solved Eqs. (B21) in an expansion in a_{WS}/R . A general solution is not possible, but we have considered several modes on a case by case basis. In each case there are terms which oscillate rapidly, arising from the behavior of $j_l(x)$ for large x ; however, these oscillatory terms turn out to be of higher order in a_{WS}/R than the lowest-order correction to the fluid frequency.

For the (1,0), (2,0), and (3,0) modes, we find that the lowest-order correlation corrections to the cold-fluid frequencies are

$$\Delta \omega_{1m} = 0, \quad m=0,1, \quad (\text{B23a})$$

$$\Delta(\omega_{2m}^2) = \frac{10\mu}{M n_0 R^2}, \quad m=0,1,2, \quad (\text{B23b})$$

$$\Delta(\omega_{3m}^2) = \frac{28\mu}{M n_0 R^2}, \quad m=0,1,2,3. \quad (\text{B23c})$$

These frequency shifts agree with the predictions of perturbation theory, Eqs. (3.41), (3.44), (3.47), and (3.50), when the spherical limit $R=L$ is taken and when p is set equal to zero.

The spatial dependence of the potential can also be compared to the results of perturbation theory. For example, when lowest-order correlation corrections to the constants A/B , C/B , and G/B are kept for the (2,0) mode, one obtains

$$\frac{A}{B} = -\frac{20}{3} \frac{k_1 R}{\text{sink}_1 R} \frac{\mu}{M n_0 \omega_p^2},$$

$$\frac{C}{B} = -\frac{2R}{k_2 \text{sink}_2 R}, \quad (\text{B24})$$

and

$$\frac{G}{B} = \frac{2}{5} R^5 + \frac{10}{3} \frac{\mu}{M n_0 \omega_p^2} R^3.$$

When employed in Eqs. (B17) and (B19), these constants, together with Eq. (B23b), yield the perturbed potential $\delta\phi$ for the (2,0) mode.

Note that if either $k_1 R$ or $k_2 R$ equals $n\pi$ for any integer n , then A/B and/or C/B are not small. Physically, these resonances occur because the (2,0) surface mode couples to very short-wavelength bulk plasma and transverse sound (torsional) oscillations. When $k_1 R = n\pi$ compressional bulk plasma oscillations are driven to large amplitude by the surface mode because the plasma oscillations become resonant in the spherical plasma at $k_1 R = n\pi$ [see Eq. (B22) in the large $k_1 R$ limit]. When $k_2 R = n\pi$ transverse sound oscillations, also coupled to the surface mode by correlation effects, are resonant and are driven to large amplitude. However, these driven bulk plasma modes and sound modes are of very short wavelength since the (2,0) frequency is on the order of ω_p , so both k_1 and k_2 are of $O(1/a_{\text{WS}})$ (in a strongly correlated plasma κ and μ are of order $n_0 q^2/a_{\text{WS}}$). Such short-wavelength modes would be damped in a real plasma, so this unphysical ringing behavior can be

removed by adding small but finite negative imaginary parts to κ and μ . Now A/B and C/B become exponentially small in the fluid limit $R/a_{\text{WS}} \rightarrow \infty$.

We can compare the exact result for $\delta\phi$ from Eqs. (B24), (B23b), (B17), (3.8), and (B19) to that obtained using perturbation theory by projecting out that portion of $\delta\phi$ which is orthogonal to the cold-fluid eigenfunction ψ , given by Eq. (3.6) for $l=2$, $m=0$, and $d \rightarrow 0$:

$$\Delta\psi = \delta\phi - \psi(\psi, \delta\phi)/(\psi, \psi).$$

Carrying out the required inner products yields the following exact result for the correlation correction to the (2,0) potential in the limit $R/a_{\text{WS}} \rightarrow \infty$:

$$\Delta\psi(r, \theta) = \frac{\mu}{M n_0 \omega_p^2 R^2} \psi(R, \theta) f(r),$$

where $\psi(R, \theta)$ is the cold-fluid potential evaluated at the surface of the plasma, and

$$f(r) = \begin{cases} \frac{35}{3} \left(\frac{r}{R}\right)^2, & r < R \\ -5 \left(\frac{R}{r}\right)^3, & r > R. \end{cases} \quad (\text{B25})$$

Just as in Eq. (B9), we are able to write $\Delta\psi$ as a product of $\psi(R, \theta)$ and a dimensionless function $f(r)$. Figure 5 shows excellent agreement between the exact $f(r)$ from Eq. (B25) and the perturbation theory result of Eq. (B9).

The exact result for $f(r)$ from Eq. (B25) exhibits a boundary layer at the plasma edge. Physically, this boundary layer forms when compressional bulk plasma oscillations are coupled into the surface (2,0) plasma oscillations by correlations. Since bulk plasma modes are of short wavelength they are strongly damped in a distance of $O(1/\text{Im}k_1)$ by the small but finite imaginary contributions to κ and μ . In the fluid limit $R/a_{\text{WS}} \rightarrow \infty$, $|k_1 R| \rightarrow \infty$, and a boundary layer appears in $\Delta\psi$ that is of negligible width compared to R . The potential eigenfunction then exhibits the discontinuity displayed in the figure.

-
- [1] D. J. Heinzen, J. J. Bollinger, F. L. Moore, W. M. Itano, and D. J. Wineland, Phys. Rev. Lett. **66**, 2080 (1991); **66**, 3087(E) (1991); J. J. Bollinger, D. J. Heinzen, F. L. Moore, W. M. Itano, D. J. Wineland, and D. H. E. Dubin, Phys. Rev. A **48**, 525 (1993).
- [2] C. S. Weimer, J. J. Bollinger, F. L. Moore, and D. J. Wineland, Phys. Rev. A **49**, 3842 (1994).
- [3] M. D. Tinkle *et al.*, Phys. Rev. Lett. **72**, 352 (1994).
- [4] R. G. Greaves, M. D. Tinkle, and C. M. Surko, Phys. Rev. Lett. **74**, 90 (1995).
- [5] J. S. deGrassie and J. H. Malmberg, Phys. Rev. Lett. **39**, 1077 (1977).
- [6] D. H. E. Dubin, Phys. Rev. Lett. **66**, 2076 (1991).
- [7] D. H. E. Dubin and J. P. Schiffer, preceding paper, Phys. Rev. E **53**, 5249 (1996).
- [8] F. M. Penning, Physica **3**, 873 (1936).
- [9] W. Paul and H. Steinwedel, Z. Naturforsch. A **8**, 448 (1953).
- [10] J. J. Bollinger and D. J. Wineland, Phys. Rev. Lett. **53**, 348 (1984); L. Turner, Phys. Fluids **30**, 3196 (1987); D. H. E. Dubin, Phys. Fluids B **5**, 295 (1993).
- [11] L. R. Brewer, J. D. Prestage, J. J. Bollinger, W. M. Itano, D. J. Larson, and D. J. Wineland, Phys. Rev. A **38**, 859 (1988).
- [12] E. Wigner, Phys. Rev. **40**, 749 (1932); E. Pollock and J. Hansen, Phys. Rev. A **8**, 3110 (1973).
- [13] G. Stringfellow, H. DeWitt, and W. L. Slattery, Phys. Rev. A **41**, 1105 (1990).
- [14] D. H. E. Dubin, Phys. Rev. A **42**, 4972 (1990).
- [15] D. H. E. Dubin and T. M. O'Neil, Phys. Rev. Lett. **60**, 511 (1988); A. Rahman and J. Schiffer, *ibid.* **57**, 1133 (1986).
- [16] R. C. Davidson, *Physics of Nonneutral Plasmas* (Addison-Wesley, Reading, MA, 1990), Sec. 3.3.
- [17] S. L. Gilbert, J. J. Bollinger, and D. J. Wineland, Phys. Rev.

- Lett. **60**, 2022 (1988); G. Birkel, S. Kassner, and H. Walther, Nature (London) **357**, 310 (1992).
- [18] D. H. E. Dubin, Phys. Rev. A **40**, 1140 (1989); J. P. Schiffer, Phys. Rev. Lett. **70**, 818 (1993); D. H. E. Dubin, *ibid.* **71**, 2753 (1993).
- [19] P. M. Morse and H. Feshbach, *Methods of Theoretical Physics* (McGraw-Hill, New York, 1963), Chap. 5.
- [20] L. Landau and E. M. Lifshitz, *Theory of Elasticity*, 3rd ed. (Pergamon, New York, 1986), p. 88.
- [21] L. Landau and E. M. Lifshitz, *Theory of Elasticity* (Ref. [20]), pp. 137 and 138.
- [22] J. P. Hansen and I. R. McDonald, *Theory of Simple Liquids*, 2nd ed. (Academic, London, 1986), p. 190.
- [23] E. M. Lifshitz and L. P. Pitaevskii, *Physical Kinetics* (Pergamon, New York, 1989), pp. 17 and 245.
- [24] L. Landau and E. M. Lifshitz, *Quantum Mechanics* (Pergamon, New York, 1981), p. 133ff.
- [25] J. J. Bollinger, D. J. Wineland, and D. H. E. Dubin, Phys. Plasmas **1**, 1403 (1994).
- [26] D. Bohm and E. P. Gross, Phys. Rev. **75**, 1851 (1949).
- [27] R. L. Spencer, in *Non-neutral Plasma Physics II*, edited by J. Fajans and D. H. E. Dubin, AIP Conf. Proc. No. 331 (AIP, New York, 1995).
- [28] H. Totsuji, J. Chem. Phys. **75**, 871 (1981).
- [29] A. E. H. Love, *Some Problems of Geodynamics* (Dover, New York, 1911).